npj | materials sustainability

Review

https://doi.org/10.1038/s44296-024-00047-3

Magnetic hydrochar for sustainable wastewater management

Huishan Meng[1,2], Zhijie Chen[3] ✉, Wei Wei[2], Juan Xu[1] ✉, Haoran Duan[3], Min Zheng[3] & Bing-Jie Ni[3] ✉

Sustainable wastewater treatment requires economical, high-performance materials. Magnetic hydrochar, synthesized from low-cost feedstocks, combines tunable surface properties and magnetic functionality, enabling efficient pollutant removal, facile magnetic separation, and cost-effectiveness. This review explores recent advancements in the synthesis and application of magnetic hydrochar for wastewater treatment. Magnetic hydrochar is promising for practical wastewater treatment, as demonstrated by sustainability assessments, bridging the gap between cutting-edge technology and practical implementation in environmental remediation.

Effective wastewater management is essential for safeguarding public health and promoting environmental sustainability. Various technologies, including electro/photo-catalysis, adsorption, and advanced oxidation processes (AOPs), have been developed to address pollutants in wastewater[1,2]. The advancement of these technologies has been closely tied to the development of functional materials[3]. In addition to material performance, cost is a key factor influencing large-scale applications[4,5]. As a result, the development of cost-effective functional materials has become a priority[6–8]. Compared with the traditional functional materials, carbon-based functional materials derived from the renewable materials offer an eco-friendly alternative and can be easily modified to enhance their wastewater treatment capacity, making them efficient for a range of pollutants[9]. Inexpensive bio-feedstocks such as food waste, agricultural by-products, and industrial residues, have been developed for fabricating functional materials. Pyrolysis and hydrothermal heating are common strategies used to process these bio-feedstocks. Biochar, produced through pyrolysis at high temperatures in an oxygen-limited or oxygen-free environment, exhibits a high specific surface area and a well-developed porous structure, leading to a reduced environment impact and effective capabilities for wastewater treatment[10,11]. Otherwise, hydrothermal carbonization requires less energy due to its relatively low heating value and wet heating environment[12,13]. This process contributes to the reduction of greenhouse gas emissions and enhances the carbon content of the produced hydrochar, thereby minimizing environmental impact. The resulting hydrochar has attracted significant attention due to its low production cost and abundant surface functional groups[14–17]. The mesoporous structure, abundance of functional groups, and favorable chemical properties make hydrochar highly effective for pollutant removal. Furthermore, its tunable surface chemistry enhances its ability to target emerging contaminants[12,18].

One challenge associated with hydrochar is its efficient recovery from water systems, particularly with nano-sized particles that pose the risk of secondary pollution. To address this, magnetic hydrochar has been developed as a promising solution for wastewater treatment[19,20]. By incorporating magnetic compounds into carbon matrices, magnetic hydrochar allows for easy and cost-effective separation using an external magnetic field. This innovation retains hydrochar's adsorption and catalytic capabilities while optimizing its pore structure and enhancing active sites. Additionally, the carbon layer protects the incorporated inorganic substances from leaching during treatment. Studies demonstrate that magnetic biochar displays minimal differences from pristine biochar, which may be attributed to its larger surface area and smaller pore structure[21]. The pollutant removal mechanisms of magnetic biochar differ from those of magnetic hydrochar[22]. Economic analyses have shown that magnetic hydrochar is more cost-effective than traditional commercial activated carbon, offering a sustainable and practical approach to wastewater treatment[23]. Despite significant progress in the synthesis and application of magnetic hydrochar, a comprehensive review covering its fabrication, properties, and performance is still lacking.

In this review, we aim to fill this gap by exploring magnetic hydrochar's synthesis from various precursors, examining its physicochemical properties, and analyzing its wide applications in wastewater treatment. The combined benefits of carbon and metal-based materials position magnetic hydrochar as a highly effective and sustainable option for wastewater treatment.

Magnetic hydrochar

Magnetic hydrochar retains many of the advantageous properties of regular hydrochar while incorporating magnetic elements that significantly enhance its functionality, particularly in wastewater treatment. The magnetic components not only enable easy separation from treated water via an external magnetic field but also modify the hydrochar's physical and chemical characteristics, thereby improving its overall efficiency in pollutant

[1]School of Ecological and Environmental Sciences, East China Normal University, Shanghai, P. R. China. [2]Centre for Technology in Water and Wastewater (CTWW), School of Civil and Environmental Engineering, University of Technology Sydney, Sydney, NSW, Australia. [3]School of Civil and Environmental Engineering, The University of New South Wales, Sydney, NSW, Australia. ✉e-mail: zhijie.chen1@unsw.edu.au; jxu@des.ecnu.edu.cn; bingjieni@gmail.com

removal. This section discusses the various fabrication methods for producing magnetic hydrochar and explores the factors influencing its development, such as precursor materials and synthesis conditions. Furthermore, the key physicochemical properties of magnetic hydrochar, including porosity, surface structure, and magnetic functionality, are examined to illustrate how these attributes contribute to its superior performance in adsorption and catalysis applications.

Fabrication process

Magnetic hydrochar is synthesized through hydrothermal processing of a variety of renewable organic feedstocks, without specific restrictions on the carbon source. Lignocellulosic biomass, such as woody biomass and agriculture residue[24–26], has been identified as efficient carbon precursors for hydrochar production[27,28]. Lignocellulosic materials in organic resources contribute to an increased hydrochar yield[29]. Non-lignocellulosic substances, including non-woody biomass[30], animal manures[31], industrial residues[32], and pure organic solutions[33], underwent carbonization, which also led to the formation of hydrochar. Among these organic materials, iron-enriched organic feedstocks can be directly converted into magnetic hydrochar, whereas other organic feedstocks require the addition of magnetic precursors. Metallic precursors, including iron (Fe)[34], cobalt (Co)[35], and nickel (Ni) compounds[25], were employed to provide the magnetic properties of hydrochar. Most research has concentrated on synthesizing ferromagnetic hydrochar, due to the relatively low cost of these precursors, the strong magnetic characteristics of the resulting hydrochar, and its improved biocompatibility for ecological applications[36,37]. In these cases, magnetic hydrochar can be synthesized using either a one-step or two-step method. Figure 1 illustrates the different fabrication pathways.

Iron-rich feedstocks can be transformed into magnetic hydrochar through a one-step hydrothermal carbonization process. During hydrothermal carbonization, the Fe component is reduced by organic matter, leading to the formation of Fe_3O_4, which enhances both the wastewater treatment efficiency and the magnetic properties of the hydrochar. It has been reported that nanosized magnetite (Fe_3O_4) particles can disperse onto hydrochar through the hydrothermal carbonization of iron-rich hyperaccumulators[38]. Additionally, industrial wastes such as Chinese medicine industry waste[39], iron-enriched sludge[40], and coking sludge[41], which are rich in Fe, have been shown to facilitate the formation of magnetic hydrochar via a similar one-step process.

Magnetic hydrochar has been synthesized from various biowastes combined with external metal salts via a one-step hydrothermal process. For instance, co-precipitation of iron(III) chloride ($FeCl_3$) and iron(II) sulphate ($FeSO_4$) under alkaline conditions, followed by hydrothermal treatment with paunch waste, has been shown to produce magnetic hydrochar embedded with Fe_3O_4 nanoparticles[42]. The simultaneous incorporation of all components plays a key role in the successful synthesis of magnetic hydrochar. In another example, magnetic hydrochar was produced from Acacia koa pod covers and $FeSO_4$ in an alkaline solution through the same hydrothermal process[43]. Incorporating Fe salts in different oxidation states during hydrothermal carbonization of biowaste can result in the formation of magnetic hydrochar[44,45]. Various additives, such as metal salts with oxidative capacities[46], iron-rich waste[47], and magnetic solids[48], have also been co-hydrothermally treated with organic feedstocks, improving the carbonization and magnetization processes to yield high-quality magnetic hydrochar. However, the mechanism behind magnetic phase formation still requires further investigation.

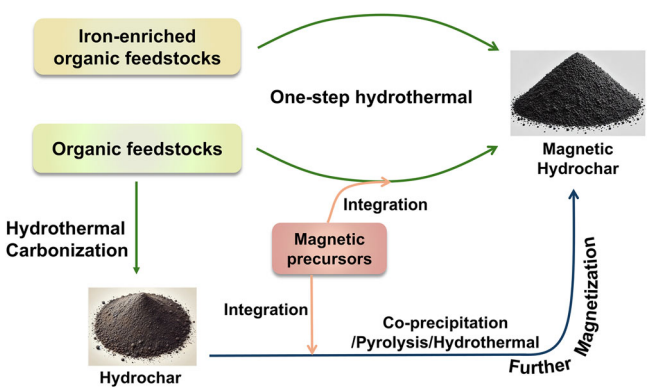

Fig. 1 | Methods for fabricating magnetic hydrochar.

Magnetic hydrochar can also be fabricated through the magnetization and activation of hydrochar. The choice between one-step and two-step hydrothermal processes plays a crucial role in determining pollutant removal efficiency[49]. Post-treatment significantly influences the physicochemical properties of magnetic hydrochar. For example, magnetic hydrochar can be synthesized by first producing hydrochar through the hydrothermal processing of glucose, followed by co-precipitation with $FeSO_4$ and $FeCl_3$ in an alkaline solution[50]. Magnetization through co-precipitation has been shown to increase the specific surface area of the hydrochar[51]. Additionally, the reduction-precipitation method can be used to create magnetic hydrochar by introducing reducing agents such as sodium sulfite[52] or sodium borohydride[25] to facilitate the formation of the magnetic phase on the hydrochar. Another approach involves subjecting hydrochar to further hydrothermal treatment with magnetic precursors, providing a straightforward method for functionalizing the material[53]. Further hydrothermal treatments serve as an efficient means to enhance the properties of magnetic hydrochar[54].

Although hydrochar contains abundant functional groups, its relatively low surface area and poor porosity limit its broader environmental applications. To address this, simultaneous magnetization and activation of hydrochar have been explored to optimize its properties. For example, the porous structure of hydrochar has been shown to improve after the pyrolysis of rice husk-based hydrochar in the presence of $FeCl_3$ and zinc chloride ($ZnCl_2$)[55]. In this process, $ZnCl_2$ acts as an activation agent, creating pores and enhancing the surface area. The production of efficient magnetic hydrochar can be achieved by adjusting activation agents, such as carbon dioxide[56], potassium hydroxide[30], and various types of iron salts[57,58], during the magnetization and activation stages. Furthermore, post-pyrolysis treatment of magnetic hydrochar has been found to improve corrosion resistance in acidic environments and enhance magnetic properties, providing additional benefits for environmental applications[59].

Based on the reviewed synthesis methods, magnetic hydrochar can be produced through relatively simple procedures. The fabrication of magnetic hydrochar using a wide range of organic and inorganic feedstocks, along with various synthesis approaches, has been extensively studied. These efforts aim to optimize the process and enhance the performance of magnetic hydrochar for wastewater treatment applications. The key factors influencing the fabrication process will be discussed in the following section.

Properties of magnetic hydrochar

Hydrochar produced through hydrothermal carbonization shows enhanced carbon content and lower H/C and O/C ratios compared to its organic feedstocks. Magnetizing hydrochar tends to increase both carbon and ash content while also raising its aromaticity. The ash in magnetic hydrochar is generally rich in Fe, along with other inorganic elements such as Mn and Co. High levels of carbonization in magnetic hydrochar have been found to significantly improve catalytic efficiency in the Fenton process[60]. X-ray photoelectron spectroscopy (XPS) and Fourier transform infrared spectroscopy (FTIR) were employed to identify the chemical states of surface elements. The aromatic structure present on the magnetic hydrochar facilitated pollutant adsorption through π-π interactions[61]. The abundant oxygen-containing functional groups (OFGs) in magnetic hydrochar significantly improved its adsorption and catalytic performance[47,62]. The point of zero charge (pH_{PZC}) of magnetic hydrochar, influencing electrostatic interactions with pollutants, is shaped by its surface chemical properties. Research has demonstrated that acidic functional groups reduced the pH_{PZC}

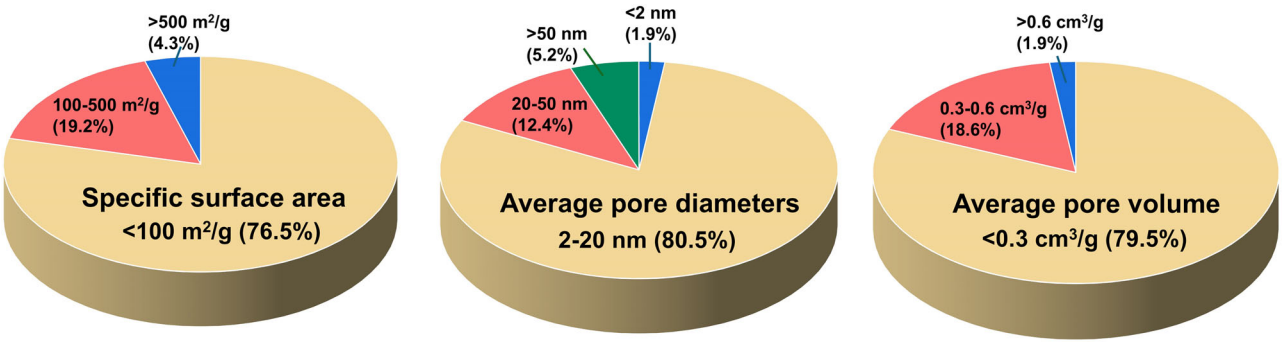

Fig. 2 | Structural properties of magnetic hydrochar (Data collected from Google Scholar up to November 2024; sample sizes: 187 for specific surface area, 154 for average pore diameter, and 156 for average pore volume).

of magnetic hydrochar from 7.35 to 6.55[31]. Its surface chemical properties significantly influence both adsorption and catalytic performance.

Magnetic particles can be distributed either on the surface or embedded within the carbon matrix in the magnetic hydrochar, depending on the fabrication methods and variations in magnetic precursors[34,63]. Fe species in magnetic hydrochar were primarily held by chemical bonds rather than simple physical cohesion[64], which enhance electron transfer when functioning as a catalyst. Carboxyl (-COOH) and hydroxyl groups (-OH) on hydrochar interacted with magnetite nanoparticles through coulombic force[53]. Additionally, it has been suggested that the carbon matrix prevented the agglomeration of metallic nanoparticles, resulting in a high dispersion of magnetic nanoparticles on the surface[65]. Iron species encased within carbon layers exhibited strong acid resistance, while non-magnetic materials may reduce saturation magnetization.

The stronger magnetism of magnetic hydrochar improves its separation efficiency from the treatment solution. The formation of magnetic inorganic particles, such as ferrites, zero-valent Fe/Ni, and metal oxides, is the primary source of magnetism in hydrochar. Saturation magnetization (Ms), measured by a vibrating sample magnetometer and analyzed through hysteresis loops, was used to indicate the magnetism of hydrochar[39]. Materials with an Ms > 1 emu/g are considered highly magnetic and suitable for magnetic separation. Variations in the type and concentration of inorganic species led to differences in saturation magnetization[31,66]. Fe_3O_4 was a commonly identified component in magnetic hydrochar, as revealed by FTIR and XPS analyses. Fe_3O_4 possesses high saturation magnetization, although its acid resistance is relatively lower than that of γ-Fe_2O_3[63]. Uniformly dispersed magnetic particles on hydrochar demonstrate efficient and stable interactions with the carbon matrix, promoting electron transfer and enabling catalyst recovery during wastewater treatment.

Magnetic hydrochar exhibited a range of morphologies, including bulk, layered, spongy, and spherical forms[67–69]. It retained the uneven, porous structure of hydrochar, with enhanced porosity and surface roughness, and was uniformly coated with inorganic particles[53]. Furthermore, smooth carbon spheres with magnetic particles attached to their surfaces were observed in magnetic hydrochar synthesized from organic wastewater[65]. The size of the magnetic hydrochar ranges from nanoscale to microscale, with magnetic particles predominantly distributed at the nanoscale. The diverse morphologies and structural characteristics of magnetic hydrochar determine its specific surface areas and pore properties. Figure 2 illustrates the distribution of specific surface areas and pore structures.

The specific surface area of most magnetic hydrochar is generally below 100 m^2/g, likely due to the constraints of low hydrothermal temperatures and solution conditions during synthesis. Therefore, further high-temperature pyrolysis can result in a specific surface area exceeding 500 m^2/g, and in some cases, reaching up to 973.56 m^2/g[30]. The pore structure of magnetic hydrochar predominantly fell within the mesopore range (2 nm to 20 nm), while both micropores (pore diameter < 2 nm) and macropores (pore diameter > 50 nm) are also present in smaller quantities[70,71]. The average pore volume remains below 0.3 cm^3/g. Specific surface areas and pore volumes affect the capacity for pollutant treatment, while pore diameters influence pollutant entry and diffusion, impacting both adsorption and catalysis.

Various carbon-based materials have been applied in wastewater treatment, each with distinct characteristics. Biochar, known for its substantial specific surface area, has proven to be a promising material[72]. Hydrochar possesses numerous functional groups[73], while magnetic hydrochar features a multifunctional surface, a mesoporous structure, and integration with inorganic components, offering significant potential for wastewater treatment.

Influencing factors by the fabrication parameters

The production of functional carbon materials largely depends on the properties of the precursor, activation conditions, and processing parameters[74]. Likewise, the fabrication of magnetic hydrochar is significantly influenced by the choice of organic feedstock, the selection of Fe precursors, and specific process conditions. Each of these factors plays a critical role in determining the chemical and structural characteristics of the resulting magnetic hydrochar.

Feedstocks. The physicochemical structure of hydrochar is largely influenced by the chemical properties of the feedstock[75]. For example, a study comparing magnetic hydrochar derived from sunflower husk and orange juice residue found that the magnetic hydrochar from orange juice residue (MHC_{OR}) exhibited a higher BET surface area and smaller pore diameter compared to that from sunflower husk (MHC_{SFH})[76]. Additionally, the chemical structure was altered due to the differences in biomass feedstocks, with MHC_{OR} demonstrating a higher capacity for removing malachite green. The distinct components in organic feedstocks optimized both the carbon and magnetic inorganic structures of the resulting materials. Magnetic hydrochar was synthesized by co-precipitating iron precursors with hydrochar derived from egg white and sucrose[77]. Sucrose played a key role in forming the hydrochar framework, where higher sucrose content led to a morphological transition from layered to spherical structures.

It has also been reported that reducing sugars, such as glucose in the feedstock, facilitate the formation of magnetic Fe_3O_4 rather than Fe_2O_3 during one-step synthesis[78]. Fe_3O_4 exhibits strong ferromagnetic properties, ensuring sufficient magnetic separation capability for hydrochar. This was further supported by findings where glucose reacted with Fe(III) during a one-step hydrothermal process, leading to the formation of Fe_3O_4[79]. The concentration of glucose significantly influenced the morphology and size of the magnetic hydrochar nanocomposites. A synergistic effect between carbohydrates and proteins was also observed during the hydrothermal treatment of sewage sludge, which enhanced the formation of magnetic Fe_3O_4[80]. Moving forward, more attention should be given to the co-existing components and the proportion of specific elements in organic feedstocks to design more efficient magnetic hydrochar.

Magnetic precursors. The magnetic properties of most magnetic hydrochar originate from the addition of inorganic compounds. The formation of magnetic Fe_3O_4 depends on the specific types of iron salts used. Studies have indicated that Fe(III) plays a critical role in the synthesis of iron carbide, while the combined addition of Fe(III) and Fe(II) favors the formation of magnetic Fe_3O_4[66]. The presence of Fe(II) promotes the formation of highly magnetic Fe_3O_4. Co-hydrothermal treatment with $Fe_2(SO_4)_3$, sewage sludge, and glucose produced magnetic hydrochar with strong magnetic separation capability, enhanced by the reducing properties of glucose[78]. The use of high $FeCl_3$ concentrations was shown to facilitate the hydrolysis of organic substances, resulting in increased saturation magnetization[81].

The introduction of inorganic substances during the hydrothermal process significantly also alters the carbonization pathways of the organic material, thereby influencing the chemical composition and pore structure of the resulting magnetic carbon[82]. For instance, the addition of ferric sludge during the hydrothermal carbonization of biological sludge has been shown to inhibit pore development, leading to a reduction in pore size[60]. The use of strong oxidizing agents like K_2FeO_4 resulted in magnetic hydrochar with a high specific surface area, larger pore volume, and an increased presence of oxygen-containing functional groups following hydrothermal processing with organic feedstocks[24]. Additionally, studies comparing various iron salts in the synthesis of magnetic hydrochar via a two-step process revealed that $FeCl_3$ is particularly effective in producing high-porosity, acid-resistant magnetic hydrochar from sawdust. Other iron salts, such as FeC_2O_4, $Fe(C_4H_5O_7)$, and $Fe_2(SO_4)_3$, were found to hinder pore structure development due to reduced carbonization[63]. Magnetic hydrochar synthesized with high Fe concentrations via co-precipitation demonstrated improved adsorption capacity and stability, underscoring the importance of iron salt selection in optimizing the performance of magnetic hydrochar[83].

Additional functionalization agents. Further activation and modification present promising methods for fabricating functional materials that contribute to sustainable wastewater management. Alkalis are commonly employed for activating hydrochar[84]. In one study, the etching of pharmaceutical industry waste under alkaline hydrothermal conditions demonstrated that alkali treatment not only removed organic matter and ash from the hydrochar but also enhanced its porosity and surface area[32], while introducing oxygen-containing groups and Fe_3O_4 into the magnetic hydrochar. Acid-assisted hydrothermal treatment facilitates the reduction of Fe(III) and modifies the surface functional groups on magnetic hydrochar, thereby enhancing its applicability[85].

The incorporation of additional surface functional groups can significantly improve the adsorption capacity of magnetic hydrochar for specific pollutants. Nitrogen-containing substances, such as urea, diethylenetriamine, and ethylenediamine, have been used to modify magnetic hydrochar, further enhancing its functionality[33,86,87]. Similarly, sulfur-doped magnetic hydrochar has been produced by introducing sulfur compounds like chlorosulfonic acid and carbon disulfide, which improve pollutant adsorption[69,88]. Grafting organic substances with specific functional groups onto magnetic hydrochar has also been shown to enhance its pollutant removal capabilities. For example, magnetic hydrochar functionalized with silymarin, chitosan, and β-cyclodextrin has demonstrated improved adsorption and catalytic performance in removing pollutants[89–91]. Additionally, metal oxides such as manganese dioxide (MnO_2) and calcium oxide (CaO) have been anchored onto magnetic hydrochar, resulting in structural changes that influence its adsorption capacity[92,93]. The combination of magnetic hydrochar with other metal oxides has also been found to significantly enhance its catalytic activity, further expanding its potential for environmental applications[94,95].

Temperature. Fabrication conditions, particularly temperature, heating methods, and the choice of synthesis methods, influence the structural and chemical properties of magnetic hydrochar, determining its adsorption and catalytic capabilities. Compared to hydrothermal duration and initial solution pH[96], the hydrothermal temperature has a more pronounced effect on the transformation of organic and inorganic precursors during synthesis[97], resulting different physicochemical structure. It has been found that high temperatures accelerated the carbonization of organic feedstock, producing higher carbon content and an abundance of aromatic functional groups[64]. Correspondingly, the surface morphology of magnetic hydrochar may be altered, contributing to a higher specific surface area and larger pore volume. Excessive carbonization at higher temperatures reduced the specific surface area and pore volume due to coke formation and the accumulation of ash. The bond strength between iron and other elements improved with increasing temperature, enhancing the stability of the magnetic hydrochar. Elevated temperatures promoted the conversion of Fe-containing precursors into magnetic Fe_3O_4 during the synthesis[41]. The functional groups and iron oxides formed on magnetic hydrochar, which are influenced by the hydrothermal temperature, result in varying adsorption and activation properties[35,46]. Furthermore, high temperatures enhance the crystallinity of magnetic species and reduce the impact of organic substances on magnetic properties, leading to increased saturation magnetization. In a two-step hydrothermal process, it was demonstrated that maintaining a low hydrothermal temperature is essential for producing magnetic hydrochar composites with high porosity, minimized Fe leaching, and suppressed graphitization. These temperature-controlled conditions play a key role in optimizing the structural and functional characteristics of magnetic hydrochar for enhanced performance in environmental applications[98].

Heating technology. Microwave-assisted heating has been employed during hydrothermal processing to reduce energy consumption while impacting the structural properties of the resulting material[99]. For instance, the use of microwave-assisted hydrothermal synthesis was found to reduce the yield of magnetic hydrochar compared to traditional methods, as observed in one-step microwave hydrothermal synthesis[100]. However, microwave assistance enhanced the disintegration of organic components, leading to a highly porous structure and the formation of distinct functional groups on the magnetic hydrochar. This method has shown improved efficiency in removing metal ions and organic pollutants, making it a promising approach for fabricating functional magnetic hydrochar for environmental applications[101].

Synthesis methods. The selection of synthesis procedures significantly influences the properties of magnetic hydrochar, dictating the associated energy consumption and environmental impact[102,103]. The one-step hydrothermal carbonization method requires fewer operational steps and lower energy input. Moreover, inorganic substances act as catalysts in the hydrothermal carbonization of organic matter, facilitating the formation of well-structured magnetic hydrochar optimized for wastewater treatment[64]. This method resulted in higher magnetic particle loading on hydrochar compared to the two-step synthesis method, yielding uniformly dispersed spherical magnetic particles within a carbon matrix that prevents Fe leaching[34]. In contrast, the two-step process, which combines hydrothermal carbonization with post-impregnation, led to lower Fe loading and surface aggregation of Fe particles.

Magnetic hydrochar produced by the one-step method demonstrates superior catalytic activity and stability in wastewater treatment, with reduced environmental impact. While the two-step synthesis requires more energy, it allows for tailored functional properties through precise control of various operating parameters[83,103]. For instance, magnetic hydrochar synthesized by hydrothermal carbonization followed by post-pyrolysis exhibited a large specific surface area, leading to a high adsorption capacity for As(V) in a single adsorption cycle[31].

The complex and heterogeneous nature of feedstocks, combined with the inherent variability of hydrothermal reactions, results in magnetic hydrochar with diverse properties and performance. This variability presents challenges in achieving precise control over the characteristics of

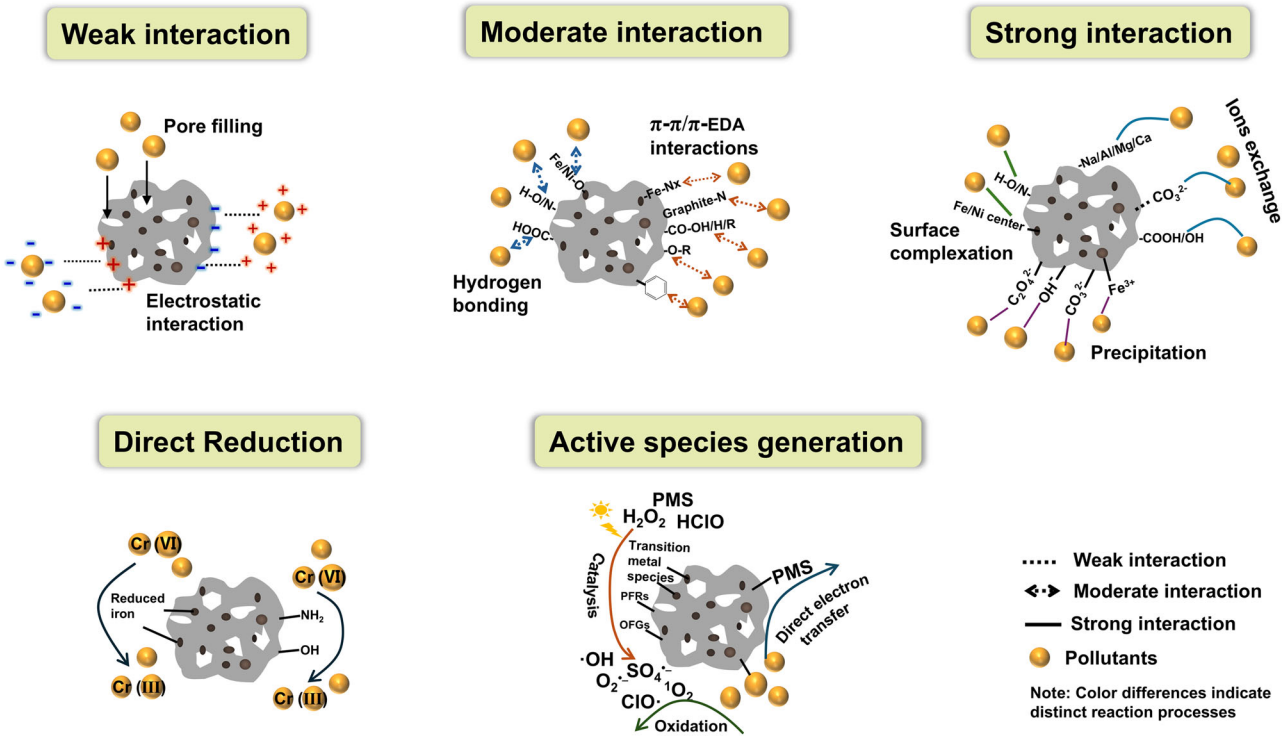

Fig. 3 | Pollutant removal mechanism of magnetic hydrochar.

magnetic hydrochar. To address this, further research is needed to comprehensively understand the effects of fabrication conditions. Despite these challenges, the flexibility of magnetic hydrochar synthesis allows for its application in treating a wide range of complex wastewater, making it a versatile solution for environmental management.

Applications in wastewater management

The combination of abundant functional groups and the porous nature of magnetic hydrochar enhances its effectiveness in pollutant adsorption and redox processes during wastewater treatment. Pollutant removal efficiency may vary based on the specific properties of magnetic hydrochar and the nature of pollutants present, as different removal mechanisms are involved. Clarifying the pollutant removal mechanism of magnetic hydrochar and identifying the key role of its properties are crucial for optimizing pollutant removal efficiency[104]. Figure 3 provides the specific adsorption mechanism for pollutant removal by magnetic hydrochar.

Pollutant adsorption mechanism on magnetic hydrochar

Organic and metal ion pollutants can be efficiently removed by adsorption onto magnetic hydrochar. Mechanisms of adsorption include pore filling, electrostatic forces, hydrogen bonding, π-π stacking, surface complexation, ion exchange, and precipitation, each contributing with different levels of interaction strength.

The porous structure of magnetic materials enhances pollutant adsorption by the pore-filling effect. A decrease in surface area and pore volume following the adsorption of pollutants like tetracycline underscored the significance of pore filling in this process[57]. Additionally, a positive correlation has been noted between the maximum adsorption capacity of magnetic materials and their surface area and micropore volume[105]. Magnetic hydrochar, with its abundant mesoporous structure, provides internal sites for pollutant adsorption via this pore-filling mechanism.

Electrostatic attraction also plays a crucial role in the physical adsorption process of magnetic hydrochar. The surface charge of magnetic hydrochar is closely related to its surface functional groups and the pH of the solution, as indicated by its point of pH_{PZC} value. When the aqueous pH exceeds the pH_{PZC}, deprotonation of oxygen-containing functional groups creates a negatively charged surface that enhances the adsorption of cations. Conversely, at pH values below the pH_{PZC}, the surface becomes positively charged, enhancing electrostatic repulsion and reducing the adsorption of cationic pollutants. Qiu's research demonstrated the significance of electrostatic interactions, showing that anionic surfactants compete with anionic Congo red for adsorption on magnetic hydrochar[106].

Chemical adsorption emerges as the dominant mechanism for pollutant removal, as indicated by the adsorption kinetics analysis of pollutants on magnetic hydrochar. This process includes hydrogen bonding, π-π interactions, surface complexation, ions exchange, and precipitation, suggesting moderate to strong interactions between pollutants and hydrochar. Chemical adsorption mechanisms were explored by examining significant alterations in the chemical states of the adsorbent before and after adsorption, providing insights into the nature of these interactions.

Hydrogen bonding and π-π interactions have been identified as key mechanisms for moderately binding pollutants to magnetic hydrochar. Hydrogen bonds are formed due to the oxygen (O)/nitrogen (N)-containing groups on the magnetic hydrochar, as indicated by changes in the FTIR peaks associated with O-H/N-H groups, and shifts in O1s/N1s peaks observed in the XPS analysis[54,92]. Additionally, Fe-O and Ni-O groups on the magnetic hydrochar act as active sites for hydrogen bond formation, further facilitating pollutant adsorption[54]. π-π and π-electron donor-acceptor (EDA) interactions are also confirmed as important adsorption mechanisms, evidenced by shifts in the binding energy of C 1s peaks and alterations in the stretching vibrations of aromatic C = C bonds[54,107]. These interactions involve electron transfer between pollutants and the magnetic hydrochar. Density functional theory (DFT) calculations have supported the presence of strong π-π interactions between dye molecules and magnetic hydrochar, based on analyses of equilibrium configurations and partial density of states (PDOS)[58]. Aromatic groups, along with functional groups such as carboxyl, carbonyl (C = O), ether groups (C-O-C), can participate in conjugated adsorption reactions with pollutants through π-π or π-EDA interactions[108]. Graphitic N and Fe-NX structures further support pollutant adsorption by intensifying π-π interactions. This effect stems from a reduction in electron cloud density and an increase in π-electron acceptor capacity in the carbon framework[109].

Magnetic hydrochar exhibits strong interactions with adsorbed pollutants, primarily through mechanisms such as surface complexation, ion exchange, and precipitation. The coexistence of inorganic and organic components on magnetic hydrochar allows for surface complexation with organic or metal ion pollutants during wastewater treatment. Competition for adsorption sites can arise, as observed in cases where organic molecules like ethylenediaminetetraacetic acid (EDTA) and tetracycline competed for binding to metal centers on the adsorbent, triggering complexation reactions[57]. The functional groups in organic pollutants, acting as soft and hard bases, can form complexes with metal ions such as Ni(III) (borderline acid) and Fe(III) (hard acid) through acid-base interactions or strong coordination bonds[54]. For the removal of inorganic ions in wastewater, functional groups containing oxygen and nitrogen readily form complexes with heavy metals[101,110]. Additionally, the strong affinity of Fe oxides in magnetic hydrochar enhances metal ion complexation during the adsorption process[111]. The lone pair electrons in oxygenous/nitrogenous groups facilitate coordination with metal ions[112].

Ion exchange and co-precipitation have been widely identified in the adsorption of ionic pollutants. During the adsorption process, functional groups such as -OH and -COOH, along with protonated iron oxides, facilitate cation exchange with pollutants like protonated tetracycline[46]. However, the inorganic components of magnetic hydrochar, such as carbonate ions (CO_3^{2-}) and metal ions like aluminum (III), calcium (II), magnesium (II), and sodium (I), are primarily responsible for driving the ion exchange process[106,113]. Xu et al. investigated that magnetic hydrochar derived from red mud engaged in ion exchange during the adsorption of pollutants, while magnetic hydrochar synthesized with $FeCl_3$ does not exhibit ion exchange in the removal of chromium ions(Cr(III))[114]. The presence of aluminum (III) in red mud promoted ion exchange with Cr(III) due to their similar spatial structure and ionic size. X-ray diffraction revealed newly adsorbed compounds on the magnetic hydrochar[70], while ions exchanged from the material were found in the aqueous solution[115]. In addition to ion exchange, metal cation pollutants can be precipitated through reactions with selected compounds on magnetic hydrochar. The Fe(III) present in the magnetic hydrochar is capable of binding with lead ions (Pb(II)) and Cr(III), leading to the formation of stable precipitates[101,109]. Furthermore, precipitates such as lead(II) oxalate ((PbC_2O_4), cadmium carbonate ($CdCO_3$) or cadmium hydroxide ($Cd(OH)_2$) have been identified in the utilized magnetic hydrochar, caused by the associated anions on its surface[110]. These reactions contribute significantly to the pollutant removal efficiency of magnetic hydrochar in wastewater treatment.

In the adsorption process, multiple mechanisms often work together to achieve effective pollutant removal, with the dominant mechanism depending on the specific characteristics of the pollutants and the conditions of the wastewater. To optimize adsorption capacity and enable selective removal of pollutants, the physicochemical structure of magnetic hydrochar should be precisely engineered based on the specific application. This precise engineering ensures that the material's surface structure, pore size, functional groups, and overall composition are optimized to target specific contaminants efficiently.

Adsorption performance of various pollutants

Investigations into the adsorption mechanism indicate that the adsorption capability of magnetic hydrochar is primarily determined by its surface functional groups rather than its specific surface area. Magnetic hydrochar has been observed to achieve an adsorption efficiency of over 90%, significantly outperforming activated carbon (below 78%) for pesticide removal, even though activated carbon features a larger specific surface area[116]. Magnetic elements and functional groups in the hydrochar improve its adsorption capacity[117]. However, the overall effectiveness remains dependent on the specific characteristics of target pollutants. Table 1 summarizes the adsorption performance for different pollutants.

Magnetic hydrochar demonstrates high adsorption efficiency and ease of recovery in dye wastewater treatment[21]. While it effectively removes a range of dyes, the adsorption process may vary under different conditions[92,118]. Qiu et al. studied the selective adsorption of Congo Red (CR) with magnetic hydrochar in the presence of other pollutants[106]. The larger molecular structure of coexisting pollutants hindered CR adsorption due to spatial limitations. The impact of organic pollutant structure and size on adsorption performance has also been discussed in other studies[54,105]. Importantly, synergy and competition in adsorption were observed between CR and coexisting organic substances, influenced by their surface charge in solution. For ionic pollutants, their surface charge in aqueous solutions dictates their adsorption performance on magnetic hydrochar. Cationic pollutants enhance the adsorption of anionic CR due to their strengthened electrostatic interactions. In contrast, anionic pollutants significantly inhibit CR adsorption competitive adsorption for positively charged active sites. Studies also indicate that modified magnetic hydrochar can achieve selective adsorption of oppositely charged ionic pollutants, with pH adjustments playing a key role in this process[87]. Pollutants with similar adsorption mechanisms compete for adsorption sites on the magnetic hydrochar, reducing the adsorption capacity for target pollutants.

Organic pollutants containing π-structures, such as TC, interact with magnetic hydrochar primarily through π-π or π-EDA interactions. In this mechanism, TC serves as both an electron donor and acceptor[108]. For methylene blue (MB) and methyl orange (MO) adsorption, MB acts as an electron acceptor, while MO acts as an electron donor. Magnetic hydrochar shows stronger electron transfer and reactivity with MB than with MO[58]. Consequently, organic pollutants with varying physicochemical properties could be selectively removed from the co-existence solution.

In addition to its ability to adsorb organic pollutants, magnetic hydrochar has also been extensively used in the treatment of metal ions. Differences in the physical and chemical properties of pollutants result in distinct adsorption processes on magnetic hydrochar[113,119]. Both metal ions and organic pollutants are typically adsorbed through weak interactions. Organic pollutants are mainly adsorbed via hydrogen bonding, π-π/EDA interactions, and surface complexation, while metal ions are primarily adsorbed through electrostatic interactions, surface complexation, ion exchange, and precipitation. Research on the removal of cadmium (Cd) ions and chlortetracycline (TCT) in a binary system found that at lower Cd(II) concentrations, TCT removal was enhanced due to reduced electrostatic repulsion, facilitated by the coordination of Cd(II) with TCT[111]. However, as Cd(II) concentrations increased, competition for complexation sites intensified, reducing the removal efficiency for both TCT and Cd(II). Zhang et al. developed magnetic hydrochar for the simultaneous adsorption of Cd(II) and anthracene, as their distinct adsorption mechanisms prevented competitive interactions[120]. Optimizing the specific adsorption mechanisms for each pollutant can improve selective removal in treatment processes.

The adsorption of metal ions on magnetic hydrochar involves various mechanisms. Factors such as ionic radius, electronegativity, and hydration energy influence the adsorption behavior of metal ions[121]. Meanwhile, the adsorption efficiency of metal ions depends on their affinity for the functional groups on magnetic hydrochar[110]. For example, the adsorption of As(V) occurs through multiple synergistic mechanisms, including pore filling, electrostatic attraction, hydrogen bonding, and complexation[31]. Magnetic hydrochar, containing lone pair electrons, facilitates interactions with aqueous arsenic (As) anions. A recent study has shown that iron oxide species, rather than organic oxygen-containing groups, played the primary role in coordinating with As(V) anions[96]. Further surface functionalization of magnetic hydrochar has been demonstrated to enhance As(V) adsorption via complexation mechanisms[122].

The removal of lead (Pb) and cadmium (Cd) ions by magnetic hydrochar is highly efficient, owing to its mesoporous structure and surface functionalization, with ion exchange, surface complexation, and precipitation being the dominant processes involved[38,123]. Studies on Pb(II) removal have highlighted that surface complexation was the primary mechanism of aminated magnetic hydrochar, while ion exchange dominated in systems enriched with inorganic compounds[70,115]. The adsorption behavior of metal ions can be tuned through surface-functionalized magnetic hydrochar, offering the potential for selective pollutant adsorption. Sulfur-modified

Table 1 | Applications of magnetic hydrochar for pollutant adsorption

Pollutants	Hydrochar	Feedstocks	Synthesis methods	Performance	Adsorption features	Ref.
Rhodamin B (RhB)	Fe-modified hydrochar	Wheat straw, $FeCl_3$	Hydrothermal carbonization-precipitation	• Removal efficiency: 91% • Experiment conditions: 5 mg/L RhB, 1 g/L adsorbent, initial pH 6, 90 min • Highest adsorption capacity: 80 mg/g • After three adsorption - desorption cycles, the RhB adsorption capacity: 2.55 ± 0.22 mg/g	Physical and chemical adsorption	21
Malachite green (MG) and methylene blue (MB)	MHC/Mn	Citrus peel, $FeCl_3$, and $KMnO_4$	Hydrothermal synthesis-chemical modification	• Removal efficiency: 97.57% (MG), 89.62% (MB) • Experiment conditions: 300 mg/L MG, 0.4 g/L adsorbent, pH 4, 420 min (MG); 50 mg/L MB, 0.8 g/L adsorbent, pH 10, 120 min (MB) Highest adsorption capacity: 1402.17 mg/g (MG) and 175.63 mg/g (MB) • After four adsorption - desorption cycles, the removal rates of MG and MB: 69.29% and 85.11%, respectively	Pore filling, electrostatic interactions, hydrogen bonding, and π-π interactions	92
MB, MG, crystal violet (CV), fuchsin basic (FB)	MHC	Rhododendron foliage, $FeCl_3$, and $FeSO_4$	Hydrothermal synthesis	• Removal efficiency: 91.496% for MB, 98.496% for MG, 99.32% for CV, 92.024% for FB • Experiment conditions: 50 mg/L dye, pH 7, 25 min • Highest adsorption capacity: 81.78 mg/g for MB, 84.22 mg/g for MG, 86 mg/g for CV, 80.26 mg/g for FB • Reusability of MHC: nine cycles for CV, eight cycles for both MG and MB, and seven cycles for FB	Adsorption isotherm: Freundlich model (CV, MG) and the Langmuir model (FB, MB)	118
Congo Red (CR)	MHC-LDH	Waste poplar sawdust, iron nitrate ($Fe(NO_3)_3$), cobalt nitrate ($Co(NO_3)_2$), magnesium nitrate, and $Al(NO_3)_3$	Hydrothermal carbonization-precipitation-chemical modification	• Removal efficiency: 96.3% • Experiment conditions: 300 mg/L CR, 0.2 g/L adsorbent, pH 6, 24 h • Maximum adsorption capacity of 1668.38 mg/g • Removal efficiency after seven consecutive adsorption - desorption cycles: 81.7%	Pore-filling, electrostatic interactions, and hydrogen bonding	106
CV and tetracycline (TC)	NiFe-MOF@AHC	Sugarcane bagasse, $FeCl_3$, $Ni(NO_3)_2$	Hydrothermal carbonization	• Maximum adsorption capacity: 395.9 mg/g (CV) and 568.1 mg/g (TC) • Adsorption capacity after four adsorption - desorption cycles: decreased from 260.4 mg/g to 198.3 mg/g (CV) and from 254.0 mg/g to 106.8 mg/g (TC)	Hydrogen bonding, surface complexation, and π-π or π-EDA interactions	54
Triclosan (TCS)	MC-X-Y	Salix psammophila, $FeCl_3$, and $ZnCl_2$	Hydrothermal carbonization-pyrolysis	• Maximum adsorption capacity: 892.9 mg/g (TCS)	Micropore filling	105
Methyl orange (MO) and MB	Fe_3O_4-AMHC	Bamboo powder, $FeCl_3$, and $FeSO_4$	Hydrothermal carbonization-precipitation	• Removal efficiency after five cycles: above 99% (MB); 75% (MO) • Experiment conditions: 100 mg/L dyes, 0.8 g/L adsorbent, pH 5 (MO)/pH 11(MB) • Maximum adsorption capacity: 202.02 mg/g (MO); 148.84 mg/g (MB)	Electrostatic interactions	87

Table 1 (continued) | Applications of magnetic hydrochar for pollutant adsorption

Pollutants	Hydrochar	Feedstocks	Synthesis methods	Performance	Adsorption features	Ref.
Tetracycline	S3C7-Fe	Sewage sludge, low-rank coal, and K_2FeO_4	Hydrothermal carbonization	• Maximum adsorption capacity: 884.04 mg/g • Adsorption capacity after five regeneration cycles: reduced by 147.08 mg/g	π-π/EDA interaction, pore filling, hydrogen bonding, and cation-π complexation	108
MB and MO	Fe@PGHC	Cotton straw, $C_6H_5FeO_7$	Hydrothermal carbonization-pyrolysis	• Maximum adsorption capacity: 529.17 mg/g (MO) and 659.61 mg/g (MB)	Electrostatic interactions, hydrogen bonding, and π-π interactions	58
Pb(II) and tetracycline (TC)	Ca-MBHC	Bamboo powder, K_2FeO_4, $CaCO_3$	Hydrothermal carbonization-pyrolysis	• Maximum adsorption capacity: 475.58 mg/g (Pb(II)); 142.44 mg/g (TC)	Electrostatic interactions, reduction, ion exchange, and surface complexation (Pb(II)); hydrogen bonding, pore filling, and π-π interactions (TC)	113
Cu(II) and MB	FeNPs@HC	Pomegranate peels and iron nanoparticles	Hydrothermal carbonization	• Maximum adsorption capacity: 278 mg/g (MB); 95.24 mg/g (Cu(II)) • Removal efficiency after four cycles: 66.9% (Cu(II)); 80% (MB)	Electrostatic and π-π interactions (MB); electrostatic interaction (Cu ions)	119
Chlortetracycline (CTC) and Cd(II)	$MnFe_2O_4$-SMHC	Swine manure, $FeCl_3$, and $MnSO_4$	Hydrothermal carbonization-precipitation	Maximum adsorption capacity: 62.16 mg/g Cd(II); 752.96 mg/g (CTC) • Removal efficiency after reuse: 65.10% after seven adsorption - desorption cycles (CTC), below 60% after four adsorption - desorption cycles (Cd(II))	Hydrogen bonding, π-π EDA interactions, cation-π interactions, and pore filling (CTC); Ion exchange and precipitation (Cd(II))	111
Anthracene (ANT) and Cd(II)	β-CD@MHC	Alfalfa and $FeCl_3$	Hydrothermal carbonization-chemical modification	• Maximum adsorption capacity: 47.28 mg/g Cd(II); 60.27 mg/g (ANT) Adsorption capacity after four adsorption – desorption cycles: reduced by 22.37% (Cd(II)); 5.18% (ANT)	Complexation and electrostatic interactions Cd(II); host-guest supramolecular interactions(ANT)	120
Cd(II)	MWSHC	Watermelon seed, $FeCl_3$, $FeCl_2$	Hydrothermal carbonization	• Removal efficiency: 96.60% (Cd(II)) • Experiment conditions: 25 mg/L, 0.01 g/L adsorbent, pH 7, 300 min • Maximum adsorption capacity: 347.2 mg/g • Removal efficiency after four adsorption - desorption cycles: 88.33% (Cd(II))	Electrostatic interaction	121
Heavy metals	M-HBAP	Invasive plants alternanthera philoxeroides, $FeCl_3$	Hydrothermal carbonization	• Maximum adsorption capacity: 153.80 mg/g (Pb(II)), 144.77 mg/g (Cr(VI)), 80.58 mg/g (Cd(II)), 78.62 mg/g (Cu(II)), 50.39 mg/g (Zn(II)), and 52.83 mg/g (Ni(II)) • Adsorption capacity after five cycles: 100.56 mg/g (Pb(II)), 115.39 mg/g (Cr(VI)), 72.48 mg/g (Cd(II)), 59.34 mg/g (Cu(II)), 10.00 mg/g (Zn(II)), and 40.15 mg/g (Ni(II))	Electrostatic interaction (Cr(VI)); Precipitation (Pb(II)); Complexation and ion exchange (Cd(II), Cu(II), Zn(II), and Ni(II))	110
As(V)	Fe@THC-700	Dairy cattle manure and $Fe(NO_3)_3$	Hydrothermal carbonization-pyrolysis	• Removal efficiency: 99.95% • Experiment conditions: 50 mg/L As(V), 2 g/L adsorbent, pH 7 • Maximum adsorption capacity: 59.18 mg/g • Removal efficiency after ten adsorption - desorption cycles: 78.40%	Pore filling, electrostatic attraction, hydrogen bonding, and complexation	31
As(V)	Fe-modified hydrochar	Olive pomace, $FeCl_2$, and $FeCl_3$	Hydrothermal carbonization-precipitation	• Maximum adsorption capacity: 2.67 mg/g	Complexation	96

Table 1 (continued) | Applications of magnetic hydrochar for pollutant adsorption

Pollutants	Hydrochar	Feedstocks	Synthesis methods	Performance	Adsorption features	Ref.
As(V)	Fe_2O_3@THC	Dairy cattle manure and $Fe(NO_3)_3$	Hydrothermal carbonization	• Removal efficiency: 98.7% • Experiment conditions: 50 mg/L As(V), 2 g/L adsorbent, pH 7 • Maximum adsorption capacity: 44.80 mg/g • Removal efficiency after four regeneration cycles: 73.3% ~ 84.8%	Electrostatic attraction, hydrogen bond interactions, complexation, and ion exchange	122
Pb(II)	SOCHC	Oil industry waste, $FeCl_2$, and $FeCl_3$	Hydrothermal carbonization-precipitation	• Maximum adsorption capacity: 361.7 mg/g	Electrostatic interaction, ions exchange, and surface complex	123
Cd(II)	Magnetic hydrochar	Iron-rich Phytolacca acinosa Roxb	Hydrothermal carbonization	• Maximum adsorption capacity: 246.6 mg/g • Removal efficiency after four consecutive cycles: lower than 40%	Electrostatic attraction, surface precipitation, ion exchange, and complexation	38
Pb(II)	AHFS	Fenton sludge	Hydrothermal carbonization	• Maximum adsorption capacity: 359.83 mg/g • Removal efficiency after five cycles: 78.5%	Cation-exchange and surface complexation	70
Pb(II)	Magnetic hydrochar	Waste vinasse and red mud	Hydrothermal carbonization	• Removal efficiency: Over 95% • Experiment conditions: 25 mg/L As(V), 0.5 g/L adsorbent, pH 5.5, 120 minutes • Maximum adsorption capacity: 223.144 mg/g • Removal efficiency after five cycles: 79%	Cation-exchange, π -π interaction, precipitation and complexation	115
Pb(II), Cd(II), Cu(II), and Zn(II)	Magnetic hydrochar	Sewage sludge and $FeCl_3$	Hydrothermal carbonization, further modified with carbon disulfide	• Maximum adsorption capacities: 105.74 mg/g (Pb(II)), 38.11 mg/g (Cd(II)), 39.38 mg/g (Cu(II)), and 26.53 mg/g (Zn(II))	Electrostatic interactions, surface complexation, and ion exchange	88
Pb(II) and Cd(II)	MHC-S	Pinecone and $FeCl_3$	Hydrothermal synthesis-chemical modification	• Maximum adsorption capacities: 149.33 mg/g (Pb(II)) and 62.49 mg/g (Cd(II)) • Removal efficiency after four cycles: 78% (Pb(II)) and 90% (Cd(II))	Electrostatic interactions, ion exchange, and complexation	124

Table 2 | Applications of magnetic hydrochar for pollutant degradation

Application	Hydrochar	Feedstocks	Synthesis methods	Pollutants	Performance	Mechanism	Ref.
Reduction and adsorption	RM/HC and IS/HC	Pinewood sawdust, red mud, and $FeCl_3$	Hydrothermal carbonization	Cr(VI)	• Removal efficiency: 89.81% with RM/HC • Experiment conditions: 100 mg/L Cr(VI), 2 g/L adsorbent, pH 4, within 24 h • Maximum adsorption capacity: 375.66 mg/g (RM/HC); 337.19 mg/g (IS/HC) • Removal efficiency after five cycles: 80%	Direct reduction, co-precipitation, complexation, physical adsorption, and ion exchange	114
Reduction and adsorption	Magnetic lignin-based hydrochar	Black liquor	Hydrothermal carbonization-air stabilization	Thallium Tl(III)	• Maximum adsorption capacity: 278.9 mg/g • Removal efficiency: over 90% • Experiment conditions: 100 mg/L Tl(III), 10 mL solution, 1 g/L dosage, 12 h reaction time, wide pH range between 2 to 9	Surface precipitation, complexation, physical adsorption, chemical reduction, and ion exchange	125
Reduction and adsorption	HTCTSIP-5	Bamboo chips and $FeSO_4$	Hydrothermal carbonization- reduction precipitation-chemical modification	Cr(VI)	• Removal efficiency: 98.16% • Experiment conditions: 120 mg/L Cr(VI), 0.5 g/L adsorbent, pH 3, within 6 h • Maximum adsorption capacity: 532.35 mg/g • Adsorption capacity at sixth cycle: 122.75 mg/g	Direct reduction, electrostatic interactions, hydrogen bonding, and surface complexation	26
Reduction and adsorption	$MMHC_{QA}$	Molasses wastewater, $FeCl_3$ and $FeCl_2$	Hydrothermal carbonization-chemical modification	Cr(VI)	• Maximum adsorption capacity: 109.05 mg/g • Cycling efficiency after five adsorption-desorption cycles: over 94%	Direct reduction, electrostatic interactions, ion exchange, and surface complexation	33
Oxidation and adsorption	$NiFe_2O_4$@C	Tannery wastewater and $NiFe_2O_4$ particles	Hydrothermal carbonization	Tl(I)	• Removal efficiency: 99.6% • Experiment conditions: 300 mg/L Tl(I), 1.0 g/L adsorbent, pH 10, within 20 min • Maximum adsorption capacity: 1699 mg/g • Removal efficiency after five adsorption-desorption cycles: nearly to 100%	Oxidation, precipitation, and surface complexation	128
Fenton-like oxidation	HC	Iron-enriched sludge	Hydrothermal carbonization	Triclosan	• Removal efficiency: 90% • Experiment conditions: 4.0 mmol/L hydrogen peroxide (H_2O_2), 1.0 g/L catalyst, 10 mg/L triclosan, within 240 min • Removal efficiency after three cycles: 83.5%	Oxidation by hydroxide radicals (•OH), superoxide radicals ($O_2^{\bullet-}$), and nonradical singlet oxygen ($^1O_2$)	40
Fenton-like oxidation	FeC-S	Corn stalks and $FeCl_3$	Hydrothermal carbonization	Sulfamethoxazole (SMX)	• Removal efficiency: 92.6% • Experiment conditions: 10 mmol/L H_2O_2, pH 4.0, 50 mg/L (SMX), within 90 min • Removal efficiency after five cycles: 85.7%	Oxidation by •OH and $O_2^{\bullet-}$	130

Table 2 (continued) | Applications of magnetic hydrochar for pollutant degradation

Application	Hydrochar	Feedstocks	Synthesis methods	Pollutants	Performance	Mechanism	Ref.
Fenton-like oxidation	Sil-Fe-CBC	Clematis residues and $FeSO_4$	Hydrothermal carbonization-chemical modification	Tetracycline (TC)	• Removal efficiency: 91% • Experiment conditions: 0.4 mL H_2O_2 (30%), pH 3, 0.6 g/L catalyst, within 120 min	Oxidation by •OH radicals	89
Peroxymonosulfate (PMS) activation	$CoFe_2O_4$/hydrochar	Rice straw powder, $Fe(NO_3)_3$, and $Co(NO_3)_2$	Hydrothermal carbonization	Monochlorobenzene (MCB) and p-chloroaniline (PCA)	• Removal efficiency: 91.5% (MCB) and 97.6% (PCA) • Experiment conditions: 2 mM PMS, 0.2 g/L catalyst, 50 μM pollutants, within 60 min	Oxidation via sulfate radical ($SO_4^{\bullet-}$), •OH, and nonradical pathways (e.g., $^1O_2$, Fe (IV)/Co (IV), and direct electron transfer)	35
PMS activation	Magnetic hydrochar	Fe-enriched sludge and $CoCl_2$	Hydrothermal carbonization	Triclosan	• Removal efficiency: 98% • Experiment conditions: 2 mM PMS, 0.6 g/L catalyst, 20 mg/L triclosan, pH 3-10, within 80 min • Removal efficiency after four cycles: 90%	Oxidation via both radical (primarily •OH) and nonradical pathways ($^1O_2$ and electron transfer)	94
PMS activation	$CoFe_2O_4$/BHC-LDH	Bamboo waste, $Fe(NO_3)_3$, and $Co(NO_3)_2$	Hydrothermal carbonization-chemical modification	Ciprofloxacin (CIP)	• Removal efficiency: 98.83% • Experiment conditions: 0.4 mM PMS, 0.1 g/L catalyst, 30 mg/L CIP, within 20 min • Removal efficiency in lake water after three cycles: nearly 100%	Oxidation by $SO_4^{\bullet-}$ and $^1O_2$	95
PMS activation	2LDH-$CoFe_2O_4$@BHC	Corncob, $Fe(NO_3)_3$, and $Co(NO_3)_2$	Hydrothermal carbonization-hydrothermal modification	Tetracycline (TC)	• Removal efficiency: 100% • Experiment conditions: 0.24 mM PMS, 0.1 g/L catalyst, 15 mg/L TC, within 10 min • Removal efficiency after three cycles: nearly 70%	Oxidation by $SO_4^{\bullet-}$ and $^1O_2$	68
Photocatalysis	SMHC	Coconut shells, $FeCl_3$, and $FeCl_2$	Hydrothermal carbonization	Astrazon yellow (AY) dye	• Removal efficiency: 92.83% • Experiment conditions: 0.4% H_2O_2, 20 mg/L dye concentration, 2 g/L catalyst, within 80 min • Removal efficiency in four degradation cycles: over 90%	Oxidation by radical species, such as •OH	132
Photocatalysis	Magnetic hydrochar	Iron-enriched sludge	Hydrothermal carbonization	RhB	• Removal efficiency: 93.6% • Experiment conditions: 0.1 g/L catalyst, 100 mg/L RhB within 8 h radiation • Removal efficiency after five degradation cycles: 73.7%	Oxidation by •OH, $O_2^{\bullet-}$, and $^1O_2$	61
Photocatalysis	Fe_3O_4/BiOBr@HC	Glucose, Fe_3O_4 nanoparticles, and $Bi(NO_3)_3$	Hydrothermal carbonization-chemical modification	Carbamazepine (CBZ)	• Removal efficiency: 100% (CBZ), 67.41% (TOC) • Experiment conditions: 10 mg/L CBZ, 0.6 g/L photocatalyst, within 40 min under visible-LED light • Photocatalytic efficiency after five cycles: 100% (CBZ)	Oxidation by $O_2^{\bullet-}$, •OH, and photogenerated holes	133

magnetic hydrochar derived from sludge selectively adsorbed Pb(II) from a mixture containing Cd(II), Cu(II), and zinc ion (Zn(II)), primarily due to Pb(II)'s higher affinity for xanthate functional groups[88]. Similar selective adsorption of Pb(II) was also observed on sulfide-modified magnetic hydrochar produced from pinecones[124].

Investigations into the adsorption of various pollutants on magnetic hydrochar reveal that the unique physicochemical properties of pollutants lead to different adsorption behaviors. Customizing magnetic hydrochar to align with the specific attributes of target pollutants can significantly boost the efficiency and sustainability of wastewater treatment. Nevertheless, overcoming the challenge of competitive adsorption among pollutants with similar properties remains a major obstacle. Furthermore, research on the regeneration and disposal of spent magnetic hydrochar remains insufficient, potentially increasing environmental risks and energy costs.

Redox of pollutants mediated by magnetic hydrochar

In addition to adsorbing pollutants from wastewater, magnetic hydrochar also facilitates the chemical transformation of toxic pollutants into less harmful components. The high efficiency of magnetic hydrochar in pollutant degradation reduces the risk of secondary pollution during subsequent treatments involving spent materials. A notable example is the treatment of Cr(VI), where magnetic hydrochar participates in redox reactions, facilitating the reduction of Cr(VI) to the less toxic Cr(III)[23]. This reduction process is a crucial aspect of its pollutant remediation capabilities. Table 2 illustrates various redox transformations of pollutants using magnetic hydrochar. Understanding the redox mechanisms of pollutants is essential for advancing the design of more efficient functional materials. As shown in Fig. 3, magnetic hydrochar can directly participate in redox reactions with pollutants or act as a catalyst, generating reactive species that promote degradation indirectly. These functions are largely attributed to the specific functional groups present on the magnetic hydrochar surface.

Surface electron-donating groups, including low-valence iron, oxygen-containing functional groups (OFGs), and amino groups (-NH_2), directly participate in the reduction of metal ions, thereby aiding in the remediation of metal ion-contaminated wastewater. Low-valent metals in the hydrochar primarily act as reducing agents in the metal ion removal process[114,125]. A detailed examination showed that the decrease in Cr valence was accompanied by an increase in Fe valence[26]. Scavenging of reductive Fe(II) by 1,10-phenanthroline notably hindered the conversion of Cr(VI) to Cr(III). Furthermore, OFGs contributed to Cr(VI) reduction or acted as electron transfer carriers, facilitating electron movement between the reducing agent and metal ions in solution. The introduction of electron-donating groups, such as amino groups, boosted the reducing ability of magnetic hydrochar. In contrast, quaternary amine groups, which are electron-accepting, improved Cr(VI) adsorption but impeded its reduction to a lower oxidation state[33]. Therefore, functionalizing magnetic hydrochar provides greater flexibility, allowing for the customization of its properties to suit various wastewater treatment applications.

Pollutants can undergo indirect oxidation during AOPs, which catalyzes oxidants such as hypochlorite (HClO), hydrogen peroxide (H_2O_2), and peroxymonosulfate (PMS), leading to the generation of highly reactive oxygen species[126,127]. Extensive research has explored the catalytic function of magnetic hydrochar in removing metal ions and organic pollutants.

The synergy between magnetic transition metals and specific functional groups results in remarkable catalytic performance of magnetic hydrochar, enabling efficient pollutants oxidation[128]. Iron-enriched magnetic hydrochar was investigated as a catalyst in Fenton-like oxidation processes, involving mechanisms driven by hydroxide radicals (•OH), superoxide radicals ($O_2^{\bullet-}$), and nonradical singlet oxygen ($^1O_2$) mechanisms[40]. Hydroxyl radicals (•OH), primarily produced through iron-activated H_2O_2, accounted for 80.3% of total radical generation.

Magnetic hydrochar with higher Fe content exhibited enhanced performance in the Fenton-like reaction, where Fe(II) played a critical role in stimulating the generation of reactive species[85]. A series of comparative experiments demonstrated that the synergistic interactions between iron species and the carbon matrix significantly enhanced the Fenton-like catalytic reaction[129]. The carbon matrix shows limited ability to activate H_2O_2 for generating reactive species, mainly enhancing iron-catalyzed reactions and accumulating pollutants near active sites. The carbon matrix prevents the aggregation of nano Fe_3O_4 particles, allowing for better distribution of active sites and improved catalytic efficiency[130]. Persistent free radicals (PFRs) and electron-donating surface groups, such as amino, hydroxyl, and carboxyl groups, complex with iron species to promote the Fe(III)/Fe(II) cycle, sustaining continuous •OH generation. Additionally, functionalizing magnetic hydrochar with silymarin enhanced Fe(III) reduction, increasing Fe(II) levels and boosting •OH production for TC degradation[89]. PFRs also contributed to the formation of $O_2^{\bullet-}$. Active sites responsible for $^1O_2$ formation were likely associated with hydrochar defects or •OH transformation.

Magnetic hydrochar with both transition metals and oxygen-containing functional groups exhibits the capability to activate PMS[131], generating sulfate radicals ($SO_4^{\bullet-}$) with strong pollutant degradation potential, along with •OH. In addition to radical pathways, non-radical degradation mechanisms, such as the production of $^1O_2$, high-valence metal, and direct electron transfer, also play a significant role during PMS activation. Distinct degradation mechanisms of magnetic hydrochar were observed for monochlorobenzene (MCB) and p-chloroaniline (PCA)[35], with radical-based degradation dominating MCB removal, while PCA degradation, driven by non-radical pathways, showed less susceptibility to interference from co-existing pollutants.

Both transition metals and carbon-based materials demonstrate high efficiency in persulfate activation[94]. Cobalt (Co) and iron (Fe) were incorporated into magnetic hydrochar to enhance its potential for PMS activation, promoting the generation of radicals, singlet oxygen, and high-valent metals. Further modification of Fe/Co elements on magnetic hydrochar increased the availability of Co active sites, enhancing the removal efficiency of antibiotics through both radical and non-radical mechanisms[68,95]. Electron exchange between Fe and Co could promote the Co(II)/Co(III) cycle, ensuring stable catalytic activity. Similarly, surface-reducible functional groups like C-OH supported the transition metal redox cycle. Furthermore, C-OH contributes to PMS activation and the generation of radical. Carbonyl groups (C = O) likely facilitate electron transfer from nucleophilic PMS, leading to the generation $^1O_2$. Carbon components within magnetic hydrochar can activate PMS, facilitating pollutant degradation via direct electron transfer.

Magnetic hydrochar displays photosensitivity under light exposure and in acidic environments, generating highly reactive species, such as such as photogenerated holes (h^+), superoxide radicals ($O_2^{\bullet-}$), and •OH[132], which were crucial for the pollutants degradation. In addition to typical photosensitive catalysts like bismuth oxybromide and titanium dioxide, the incorporation of hydrochar and Fe_3O_4 can accelerate the generation of reactive oxygen species during photocatalysis[133]. Hydrochar facilitates electron transfer under light irradiation, reducing the recombination of photogenerated electrons and holes[134]. Moreover, the surface oxygen-containing groups are responsible for the absorption of solar light, leading to the production of H_2O_2 and •OH from oxygen molecules. The narrow-bandgap Fe_3O_4 can also produce h^+ and electron (e^-) under UV irradiation, contributing to organic pollutant breakdown. The photogenerated h^+ and e^- interacted with molecular oxygen, hydroxyl ions, and water, forming superoxide $O_2^{\bullet-}$, and •OH radicals. However, rapid recombination of electron-hole pairs in Fe_3O_4 can limit photocatalytic efficiency. To overcome this, citric acid (CA) was introduced to form a complex with Fe(III) on the hydrochar surface, enhancing electron transfer and photocatalytic performance[61].

Magnetic inorganic substances contribute to the catalytic properties, while functional groups facilitate electron transfer, facilitating the generation of reactive species. As a result, magnetic hydrochar modified with both transition metals and functional groups offers improved catalytic performance, enabling more efficient and sustainable wastewater treatment. Otherwise, further investigations are required to explore and expand the

potential catalytic applications of functionalized magnetic hydrochar. In advanced oxidation processes, additional chemical or energy input, along with the design and operation of complex equipment, must be carefully considered to ensure sustainable wastewater treatment.

Sustainability of magnetic hydrochar for wastewater treatment

Magnetic hydrochar has demonstrated strong potential in contaminant adsorption and catalytic oxidation. However, its practical application still faces challenges, particularly regarding cost-effectiveness and environmental sustainability. In this section, the economic feasibility and environmental impact of magnetic hydrochar are discussed.

The fabrication cost and environmental impact of magnetic hydrochar are critical factors for scaling up its practical applications. The cost of feedstock and pre-processing has been reported as economically favorable[114]. Economic analysis estimates the cost of magnetic hydrochar at 12.6 USD/kg, making it more affordable than commercial activated carbon (20 USD/Kg)[23]. The stability of hydrochar post-production is crucial for its subsequent applications, as it undergoes physicochemical changes during storage and pre-treatment stages[135]. Magnetic hydrochar exhibits enhanced stability due to the presence of inorganic components, reducing storage and transportation costs while minimizing environmental risks[59,136]. Removal efficiency of pollutants by magnetic hydrochar remained consistently high after 30 days of storage[92].

Prior to the application of magnetic hydrochar, water washing is frequently used as a pretreatment step until the rinse water reaches a neutral pH, followed by ethanol washing to remove unstable impurities[86]. Additionally, sodium hydroxide and hydrogen peroxide are employed to activate magnetic hydrochar by modifying surface functional groups[87,137]. Consideration of chemical costs and non-hazardous treatment of residual solutions is essential for a comprehensive economic and environmental risk assessment[138]. Additionally dry conditions such as oven or freeze drying were found to affect its catalytic efficiency[139]. Freeze drying preserves the structure of catalytic components, supporting the stability of magnetic hydrochar. Therefore, enhancing the stability of magnetic hydrochar is vital for improving economic benefits and reducing environmental risks. Studies have reported that hydrochar stability can be increased by optimizing fabrication and pretreatment procedures, including fabrication parameters[140,141], storage conditions[135], and the use of washing chemicals[142]. Future studies should prioritize the stability of magnetic hydrochar.

Reusability tests were conducted to evaluate the stability of magnetic hydrochar, providing insights into its economic cost and environmental impact. Typically, these tests involved 3 to 10 cycles of adsorption or catalytic experiments with repeated use of magnetic hydrochar. The pollutant removal efficiency of magnetic hydrochar across multiple cycles is presented in Table 1 and Table 2. Magnetic hydrochar consistently demonstrated high removal efficiency throughout consecutive treatment cycles, which contributes to a significant reduction in overall production costs.

The reusability of the adsorbent was assessed over multiple adsorption-desorption cycles, typically employing various desorbing agents, including acids, alkalis, organic solvents, and chelating agents[70,119,143]. The smallest chloride ions demonstrated higher desorption capacity for Pb(II) compared to nitrate and sulfate ions[123]. Alkaline solutions were particularly effective for desorbing organic pollutants, with sodium hydroxide showing the highest regeneration efficiency for toxic organophosphorus insecticides, followed by ammonium hydroxide and potassium hydroxide[116]. Sequential desorption with various agents has been used to achieve stepwise removal of different pollutants[120], enhancing the effective regeneration of magnetic hydrochar. Selecting appropriate desorbing agents and optimizing the desorption process can enhance the stability of magnetic hydrochar during long-term experiments, thereby reducing production and operational investments. In catalytic applications, magnetic hydrochar enables effective pollutant degradation, reducing the need for frequent regeneration. The continuous flow studies also have demonstrated the stability of magnetic hydrochar[68]. Previous studies have shown that the removal efficiency of magnetic hydrochar decreased by only 3.51% after long-term experiments[144].

Additionally, the inevitable leaching of magnetic hydrochar during multiple reuses should be considered, as it impacts reusability and poses potential environmental risks. The surface of magnetic hydrochar is also susceptible to partial oxidation by reactive oxygen species[129]. However, magnetic hydrochar maintains stable pollutant removal efficiency with minimal leaching of active components, resulting in cost-effectiveness and low environmental impact[133]. A solution pH exceeding 2.0 in catalytic reactions has little impact on iron leaching from magnetic hydrochar[61,105]. Moreover, iron leaching remained below the detection limit of atomic absorption spectroscopy when 0.1 M nitric acid was used as the desorption agent[119]. Furthermore, spent magnetic hydrochar shows minimal heavy metal leaching after treatment with heavy metal solutions, thereby reducing the risk of secondary pollution[88]. Therefore, the leaching from magnetic hydrochar has a negligible impact on its environmental footprint, demonstrating potential in sustainable wastewater treatment applications.

The stability of magnetic properties was evaluated following long-term experimental procedures, as this factor is critical in assessing the economic viability and environmental impact of magnetic hydrochar. A minor decline in magnetic separation efficiency was observed in reusability tests, though the magnetic hydrochar remained adequately recoverable for further applications[115]. Yan et al. reported that 85% of the spent magnetic hydrochar was still recoverable under an external magnetic field, emphasizing its practicality for wastewater treatment applications[145].

Throughout prolonged reuse studies, the accumulation of contaminants and degradation by-products on active sites leads to the progressive degradation of magnetic hydrochar, ultimately causing catalyst deactivation. Currently, few studies have reported the end-of-life management of spent magnetic hydrochar. Final disposal methods for magnetic hydrochar require careful consideration to support its commercial-scale production[146]. Common disposal options include incineration and landfilling, both of which are simple and relatively safe. Alternatively, reusing magnetic hydrochar as a catalyst, soil amendment, or construction material presents a potentially cost-effective approach. However, the long-term economic, social, and safety implications of these options must be rigorously evaluated.

Life cycle assessment revealed that biochar has a higher energy consumption compared to hydrochar, highlighting the sustainability hydrochar as an electrode catalyst[147]. A comprehensive life cycle assessment (LCA) should be conducted to evaluate the economic, social, and environmental impacts of magnetic hydrochar across all stages of wastewater treatment, promoting sustainable application in this field[148,149].

Conclusions and outlook

In conclusion, magnetic hydrochar stands out as a highly promising material for sustainable wastewater management, offering an impressive combination of adsorption efficiency, catalytic potential, and easy magnetic separation. Despite these advantages, there are critical challenges that must be addressed to fully realize its potential. Beyond conventional pollutant adsorption, the removal of emerging contaminants and microplastics remains underexplored. Coupling it with advanced water treatment technologies, such as electrocatalytic oxidation, could drastically expand its role in environmental remediation, offering a multi-functional approach to removing complex pollutants. To fully exploit the potential of magnetic hydrochar, further innovation is needed, particularly in integrating it with other functional materials. This includes modifying specific functional groups, adding high-performance catalytic components, and incorporating nanomaterials.

Refining its synthesis, particularly in co-hydrothermal processes with complex organic precursors, is a pressing priority, as these reactions are often unpredictable and can significantly affect the material's properties. A more in-depth investigation into the relationship between precursor composition, experimental conditions, and magnetic hydrochar's final characteristics is essential to ensure consistency and performance. Employing advanced analytical tools like machine learning can further optimize synthesis, allowing for precise control over its structure and surface

functionalities. For large-scale production of magnetic hydrochar, exploring efficient synthesis methods is essential. Integrating hydrothermal carbonization with advanced techniques such as humification and falsification enables the development of multifunctional materials with reduced production costs and minimized environmental impact.

Additionally, significant challenges remain in achieving scalability for magnetic hydrochar, with few examples of large-scale implementations involving magnetic hydrochar. Therefore, assessing the efficiency and reusability of magnetic hydrochar for a long-term is critical to determining its viability for actual wastewater application. Cost-effectiveness and environmental risks during long-term operation, including the regeneration of magnetic hydrochar, should be carefully evaluated. The toxicity of by-products formed during pollutant degradation must be evaluated, along with the potential for leaching of organic or metal components, to prevent secondary pollution.

High-flow, energy-efficient magnetic separation systems should also be designed to match the specific properties of the adsorbent and the characteristics of the target wastewater. Such customization will help achieve optimal separation performance and support the scalability of magnetic separation technologies in wastewater treatment. Additionally, proper management of spent magnetic hydrochar is essential to minimize energy consumption and environmental footprint. A comprehensive life cycle assessment (LCA) will be crucial to determining its environmental impact and to optimizing its cost-effectiveness for scalable, sustainable wastewater treatment. Addressing these challenges head-on will position magnetic hydrochar as a key material in the fight against water pollution, ensuring a cleaner, more sustainable future.

Data availability

No datasets were generated or analysed during the current study.

Received: 27 September 2024; Accepted: 21 December 2024;
Published online: 06 March 2025

References

1. Dewil, R., Mantzavinos, D., Poulios, I. & Rodrigo, M. A. New perspectives for advanced oxidation processes. *J. Environ. Manag.* **195**, 93–99 (2017).
2. Deng, Y. & Zhao, R. Advanced oxidation processes (AOPs) in wastewater treatment. *Curr. Pollut. Rep.* **1**, 167–176 (2015).
3. Li, Y. et al. Recent advance of atomically dispersed dual-metal sites carbocatalysts: Properties, synthetic materials, catalytic mechanisms, and applications in persulfate-based advanced oxidation process. *Adv. Funct. Mater.* **33**, 2301229 (2023).
4. Chen, Z. et al. Waste-derived catalysts for water electrolysis: circular economy-driven sustainable green hydrogen energy. *Nano-Micro Lett.* **15**, 4 (2022).
5. Chen, Z. et al. Recycling spent water treatment adsorbents for efficient electrocatalytic water oxidation reaction. *Resour. Conserv. Recycling* **178**, 106037 (2022).
6. Chen, Z., Wei, W., Chen, H. & Ni, B.-J. Recent advances in waste-derived functional materials for wastewater remediation. *Eco-Environ. Health* **1**, 86–104 (2022).
7. Chen, Z., Wei, W. & Ni, B.-J. Cost-effective catalysts for renewable hydrogen production via electrochemical water splitting: recent advances. *Curr. Opin. Green. Sustain. Chem.* **27**, 100398 (2021).
8. Chen, Z., Liu, Y., Wei, W. & Ni, B.-J. Recent advances in electrocatalysts for halogenated organic pollutant degradation. *Environ. Sci. Nano* **6**, 2332–2366 (2019).
9. Osman, A. I. et al. Methods to prepare biosorbents and magnetic sorbents for water treatment: a review. *Environ. Chem. Lett.* **21**, 2337–2398 (2023).
10. Osman, A. I. et al. Biochar for agronomy, animal farming, anaerobic digestion, composting, water treatment, soil remediation, construction, energy storage, and carbon sequestration: a review. *Environ. Chem. Lett.* **20**, 2385–2485 (2022).
11. Osman, A. I. et al. Facile synthesis and life cycle assessment of highly active magnetic sorbent composite derived from mixed plastic and biomass waste for water remediation. *ACS Sustain. Chem. Eng.* **10**, 12433–12447 (2022).
12. He, X., Zheng, N., Hu, R., Hu, Z. & Yu, J. C. Hydrothermal and pyrolytic conversion of biomasses into catalysts for advanced oxidation treatments. *Adv. Funct. Mater.* **31**, 2006505 (2021).
13. Ischia, G. et al. Advances in research and technology of hydrothermal carbonization: achievements and future directions. *Agronomy* **14**, 955 (2024).
14. Azzaz, A. A., Khiari, B., Jellali, S., Ghimbeu, C. M. & Jeguirim, M. Hydrochars production, characterization and application for wastewater treatment: a review. *Renew. Sustain. Energy Rev.* **127**, 109882 (2020).
15. Shyam, S. et al. Biomass as source for hydrochar and biochar production to recover phosphates from wastewater: a review on challenges, commercialization, and future perspectives. *Chemosphere* **286**, 131490 (2022).
16. Chen, Z., Wei, W., Ni, B.-J. & Chen, H. Plastic wastes derived carbon materials for green energy and sustainable environmental applications. *Environ. Funct. Mater.* **1**, 34–48 (2022).
17. Meng, H.-S. et al. Development of a three-dimensional photoelectrocatalytic reactor packed with granular sludge carbon photoelectrocatalyst for efficient wastewater treatment. *Sep. Purif. Technol.* **277**, 119642 (2021).
18. Gong, Y. et al. Bottom-up hydrothermal carbonization for the precise engineering of carbon materials. *Prog. Mater. Sci.* **132**, 101048 (2023).
19. Siddiqui, M. T. H. et al. Synthesis of magnetic carbon nanocomposites by hydrothermal carbonization and pyrolysis. *Environ. Chem. Lett.* **16**, 821–844 (2018).
20. Reynel-Ávila, H. E. et al. Engineered magnetic carbon-based adsorbents for the removal of water priority pollutants: an overview. *Adsorption Sci. Technol.* **2021**, 9917444 (2021).
21. Kohzadi, S., Marzban, N., Libra, J. A., Bundschuh, M. & Maleki, A. Removal of RhB from water by Fe-modified hydrochar and biochar—an experimental evaluation supported by genetic programming. *J. Mol. Liq.* **369**, 120971 (2023).
22. Wang, L., Huo, Q., Chang, Y. & Man, X. Preparation of sludge-derived spinel ferrite nanoparticles for highly efficient adsorption of Pb(II) from water: adsorption behaviour and mechanism interpretation via advanced statistical physics model. *J. Environ. Chem. Eng.* **12**, 113955 (2024).
23. Rind, I. K. et al. Magnetic nanoparticles loaded hydrochar for effective Cr(VI) removal from water: batch and column studies. *Mater. Chem. Phys.* **318**, 129077 (2024).
24. He, T., Zhou, X., Bao, Z., Fu, S. & Lin, X. Preparation of hydrochar by one-step hydrothermal carbonization with potassium ferrate-assisted activation for the removal of tetracycline in water. *J. Chem. Technol. Biotechnol.* **98**, 2039–2050 (2023).
25. Tang, Z., Deng, Y., Luo, T., Xu, Y.-s & Zhu, N.-m Enhanced removal of Pb(II) by supported nanoscale Ni/Fe on hydrochar derived from biogas residues. *Chem. Eng. J.* **292**, 224–232 (2016).
26. Wang, M. et al. Selective removal of Cr(VI) from solution by polyethyleneimine modified hydrochar loaded nanoscale zero-valent iron with high adsorption capacity. *Sep. Purif. Technol.* **329**, 125150 (2024).
27. Liu, Z., Wang, Z., Chen, H., Cai, T. & Liu, Z. Hydrochar and pyrochar for sorption of pollutants in wastewater and exhaust gas: a critical review. *Environ. Pollut.* **268**, 115910 (2021).
28. Fliri, L. et al. Identification of a polyfuran network as the initial carbonization intermediate in cellulose pyrolysis: a comparative

analysis with cellulosic hydrochars. *J. Anal. Appl. Pyrolysis* **181**, 106591 (2024).
29. Jalilian, M. et al. A review: hydrochar as potential adsorbents for wastewater treatment and CO_2 adsorption. *Sci. Total Environ.* **914**, 169823 (2024).
30. Saning, A. et al. Green and sustainable zero-waste conversion of water hyacinth (Eichhornia crassipes) into superior magnetic carbon composite adsorbents and supercapacitor electrodes. *RSC Adv.* **9**, 24248–24258 (2019).
31. Chen, H., Xu, J., Lin, H., Wang, Z. & Liu, Z. Multi-cycle aqueous arsenic removal by novel magnetic N/S-doped hydrochars activated via one-pot and two-stage schemes. *Chem. Eng. J.* **429**, 132071 (2022).
32. Liu, S. et al. Alkaline etched hydrochar–based magnetic adsorbents produced from pharmaceutical industry waste for organic dye removal. *Environ. Sci. Pollut. Res.* **30**, 65631–65645 (2023).
33. Huang, C. et al. Bis-amino modified magnetic molasses wastewater hydrochar adsorbent for chromium removal. *Surf. Interfaces* **46**, 104096 (2024).
34. Gai, C. et al. Facile one-pot synthesis of iron nanoparticles immobilized into the porous hydrochar for catalytic decomposition of phenol. *Appl. Catal. B Environ.* **204**, 566–576 (2017).
35. Yang, L. et al. Significant roles of surface functional groups and Fe/Co redox reactions on peroxymonosulfate activation by hydrochar-supported cobalt ferrite for simultaneous degradation of monochlorobenzene and p-chloroaniline. *J. Hazard. Mater.* **445**, 130588 (2023).
36. anak Erison, A. E. et al. Life cycle assessment of biodiesel production by using impregnated magnetic biochar derived from waste palm kernel shell. *Environ. Res.* **214**, 114149 (2022).
37. Siddiqui, M. T. H. et al. Fabrication of advance magnetic carbon nano-materials and their potential applications: a review. *J. Environ. Chem. Eng.* **7**, 102812 (2019).
38. Liu, T. et al. Preparation of magnetic hydrochar derived from iron-rich Phytolacca acinosa Roxb. for Cd removal. *Sci. Total Environ.* **769**, 145159 (2021).
39. Zhang, X. et al. Hydrochar magnetic adsorbent derived from Chinese medicine industry waste via one-step hydrothermal route: mechanism analyses of magnetism and adsorption. *Fuel* **326**, 125110 (2022).
40. Wang, F. et al. Unraveling the critical role of iron-enriched sludge hydrochar in mediating the Fenton-like oxidation of triclosan. *Environ. Pollut.* **321**, 121205 (2023).
41. Zhong, J. et al. Effect mechanism of iron conversion on adsorption performance of hydrochar derived from coking sludge. *Sci. Total Environ.* **898**, 165427 (2023).
42. Hedayati Marzbali, M., Hakeem, I. G. & Shah, K. In-situ production of magnetic char via rapid subcritical hydrothermal carbonisation of paunch waste. *Process Saf. Environ. Prot.* **169**, 177–185 (2023).
43. Vinayagam, R. et al. In-situ one-pot synthesis, characterization of magnetic hydrochar and its application as Fenton-like catalyst for the degradation of methylene blue dye. *Mater. Chem. Phys.* **317**, 129160 (2024).
44. Fouda-Mbanga, B. G., Velempini, T., Pillay, K. & Tywabi-Ngeva, Z. Hydrothermal development of magnetic-hydrochar nanocomposite from pineapple leaves and its performance as an adsorbent for the uptake of Mn^{2+} and reuseof the metal loaded adsorbent in latent fingerprint. *J. Saudi Chem. Soc.* **27**, 101624 (2023).
45. Sayğılı, G. A. & Sayğılı, H. Fabrication of a magnetic hydrochar composite via an in situ one-pot hydrocarbonization strategy for efficient herbicide removal. *Diam. Relat. Mater.* **128**, 109302 (2022).
46. Hang, J. et al. A super magnetic porous biochar manufactured by potassium ferrate-accelerated hydrothermal carbonization for removal of tetracycline. *J. Clean. Prod.* **435**, 140470 (2024).
47. Gu, L. et al. Co-hydrothermal treatment of fallen leaves with iron sludge to prepare magnetic iron product and solid fuel. *Bioresour. Technol.* **257**, 229–237 (2018).
48. Reza, M. T. et al. Production, characterization, and biogas application of magnetic hydrochar from cellulose. *Bioresour. Technol.* **186**, 34–43 (2015).
49. Katiyar, S. & Katiyar, R. A parametric optimization for leveraging the potential of ammonia modified magnetic pine cone hydrochar for Cr(VI) contaminated wastewater treatment. *Biocatal. Agric. Biotechnol.* **60**, 103286 (2024).
50. Zhou, X. et al. Hydrothermal synthesis of magnetic carbon microspheres for effective adsorption of Cd(II) in water. *J. Chem. Technol. Biotechnol.* **89**, 1051–1059 (2014).
51. Khataee, A. et al. Ultrasound-assisted removal of Acid Red 17 using nanosized Fe_3O_4-loaded coffee waste hydrochar. *Ultrason. Sonochem.* **35**, 72–80 (2017).
52. Kim, M., Jee, S.-C., Sung, J.-S. & Kadam, A. A. Supermagnetic sugarcane bagasse hydrochar for enhanced osteoconduction in human adipose tissue-derived mesenchymal stem cells. *Nanomaterials* **10**, 1793 (2020).
53. Patiño, A. A. B., Lassalle, V. L. & Horst, M. F. Magnetic hydrochar nanocomposite obtained from sunflower husk: a potential material for environmental remediation. *J. Mol. Struct.* **1239**, 130509 (2021).
54. Jais, F. M., Ibrahim, S., Chee, C. Y. & Ismail, Z. Solvothermal growth of the bimetal organic framework (NiFe-MOF) on sugarcane bagasse hydrochar for the removal of dye and antibiotic. *J. Environ. Chem. Eng.* **9**, 106367 (2021).
55. Zhang, S., Zhu, S., Zhang, H., Liu, X. & Xiong, Y. Synthesis and characterization of rice husk-based magnetic porous carbon by pyrolysis of pretreated rice husk with $FeCl_3$ and $ZnCl_2$. *J. Anal. Appl. Pyrolysis* **147**, 104806 (2020).
56. Qian, F. et al. Synthesis, characterization and adsorption capacity of magnetic carbon composites activated by CO_2: implication for the catalytic mechanisms of iron salts. *J. Mater. Chem. A* **4**, 18942–18951 (2016).
57. Zhang, Y. et al. Preparation of magnetic porous biochar through hydrothermal pretreatment combined with K_2FeO_4 activation to improve tetracycline removal. *Microporous Mesoporous Mater.* **343**, 112188 (2022).
58. Cheng, L., Ji, Y. & Liu, X. Insights into interfacial interaction mechanism of dyes sorption on a novel hydrochar: experimental and DFT study. *Chem. Eng. Sci.* **233**, 116432 (2021).
59. Burbano, A. A. et al. Influence of post-pyrolysis treatment on physicochemical properties and acid medium stability of magnetic carbon nanocomposites. *Biomass Convers. Biorefinery* **14**, 27871–27884 (2024).
60. Zhang, H., Xue, G., Chen, H. & Li, X. Magnetic biochar catalyst derived from biological sludge and ferric sludge using hydrothermal carbonization: preparation, characterization and its circulation in Fenton process for dyeing wastewater treatment. *Chemosphere* **191**, 64–71 (2018).
61. Li, Z. et al. Citric acid improved photocatalytic performance of iron-enriched sludge hydrochar towards organic pollutants: roles of iron species and dissolved organic matter. *Sep. Purif. Technol.* **354**, 128661 (2025).
62. Sun, X.-N. et al. Multiple roles of ferric chloride in preparing efficient magnetic hydrochar for sorption of methylene blue from water solutions. *Bioresour. Technol.* **373**, 128715 (2023).
63. Zhu, X. et al. Controllable synthesis of magnetic carbon composites with high porosity and strong acid resistance from hydrochar for efficient removal of organic pollutants: an overlooked influence. *Carbon* **99**, 338–347 (2016).
64. Wang, F. et al. Revealing carbon-iron interaction characteristics in sludge-derived hydrochars under different hydrothermal conditions. *Chemosphere* **300**, 134572 (2022).

65. Zhuang, X., Liu, J. & Ma, L. Facile synthesis of hydrochar-supported catalysts from glucose and its catalytic activity towards the production of functional amines. *Green. Energy Environ.* **8**, 1358–1370 (2023).
66. Zhang, B., Jiang, Y., Ding, Y., Zhang, J. & Balasubramanian, R. Iron-catalyzed synthesis of biowaste-derived magnetic carbonaceous materials for environmental remediation applications. *Sep. Purif. Technol.* **295**, 121321 (2022).
67. Staroń, P., Kuciakowski, J. & Chwastowski, J. Biocomposite of hydrochar and Lindnera jadinii with magnetic properties for adsorptive removal of cadmium ions. *J. Environ. Chem. Eng.* **11**, 110270 (2023).
68. Chen, H. et al. Degradation of Tetracycline through peroxymonosulfate activation with Co/Fe-LDH modified magnetic hydrochar: synergistic effect and low toxicity. *Sep. Purif. Technol.* **351**, 128023 (2024).
69. Jiang, X. et al. Magnetic seeds promoted high-density sulfonic acid-based hydrochar derived from sugar-rich wastewater for removal of methylene blue. *Environ. Sci. Pollut. Res.* **30**, 36872–36882 (2023).
70. Tong, S. et al. Recycle of Fenton sludge through one-step synthesis of aminated magnetic hydrochar for Pb^{2+} removal from wastewater. *J. Hazard. Mater.* **406**, 124581 (2021).
71. Tong, S. et al. Synthesis of magnetic hydrochar from Fenton sludge and sewage sludge for enhanced anaerobic decolorization of azo dye AO7. *J. Hazard. Mater.* **424**, 127622 (2022).
72. Fawzy, S. et al. Atmospheric carbon removal via industrial biochar systems: a techno-economic-environmental study. *J. Clean. Prod.* **371**, 133660 (2022).
73. Nicolae, S. A. et al. Recent advances in hydrothermal carbonisation: from tailored carbon materials and biochemicals to applications and bioenergy. *Green. Chem.* **22**, 4747–4800 (2020).
74. Zhang, B., Jiang, Y. & Balasubramanian, R. Synthesis, formation mechanisms and applications of biomass-derived carbonaceous materials: a critical review. *J. Mater. Chem. A* **9**, 24759–24802 (2021).
75. Wang, T., Zhai, Y., Zhu, Y., Li, C. & Zeng, G. A review of the hydrothermal carbonization of biomass waste for hydrochar formation: process conditions, fundamentals, and physicochemical properties. *Renew. Sustain. Energy Rev.* **90**, 223–247 (2018).
76. Burbano, A. A., Gascó, G., Horst, F., Lassalle, V. & Méndez, A. Production, characteristics and use of magnetic biochar nanocomposites as sorbents. *Biomass-. Bioenergy* **172**, 106772 (2023).
77. Vahdati-Khajeh, S. et al. Biocompatible magnetic N-rich activated carbon from egg white biomass and sucrose: preparation, characterization and investigation of dye adsorption capacity from aqueous solution. *Surf. Interfaces* **15**, 157–165 (2019).
78. Zhang, H. & Hay, A. G. Magnetic biochar derived from biosolids via hydrothermal carbonization: enzyme immobilization, immobilized-enzyme kinetics, environmental toxicity. *J. Hazard. Mater.* **384**, 121272 (2020).
79. Chen, M. et al. One-step hydrothermal synthesis of hydrophilic Fe_3O_4/carbon composites and their application in removing toxic chemicals. *RSC Adv.* **6**, 35228–35238 (2016).
80. Zhang, H., Xue, G., Chen, H. & Li, X. Hydrothermal synthesizing sludge-based magnetite catalyst from ferric sludge and biosolids: formation mechanism and catalytic performance. *Sci. Total Environ.* **697**, 133986 (2019).
81. Kaewtrakulchai, N. et al. Valorization of horse manure conversion to magnetic carbon nanofiber for dye adsorption by hydrothermal treatment coupled with carbonization. *Case Stud. Chem. Environ. Eng.* **9**, 100563 (2024).
82. Peng, X.-X., Gai, S., Liu, Z., Cheng, K. & Yang, F. Effects of Fe^{3+} on hydrothermal humification of agricultural biomass. *ChemSusChem* **17**, e202301227 (2024).
83. Di Caprio, F., Altimari, P., Astolfi, M. L. & Pagnanelli, F. Optimization of two-phase synthesis of Fe-hydrochar for arsenic removal from drinking water: effect of temperature and Fe concentration. *J. Environ. Manag.* **351**, 119834 (2024).
84. Tkachenko, V., Marzban, N., Vogl, S., Filonenko, S. & Antonietti, M. Chemical insights into the base-tuned hydrothermal treatment of side stream biomasses. *Sustain. Energy Fuels* **7**, 769–777 (2023).
85. Xu, X. et al. Treatment of industrial ferric sludge through a facile acid-assisted hydrothermal reaction: focusing on dry mass reduction and hydrochar recyclability performance. *Sci. Total Environ.* **869**, 161879 (2023).
86. Khan, M. A. et al. Heteroatom-doped magnetic hydrochar to remove post-transition and transition metals from water: synthesis, characterization, and adsorption studies. *Chemosphere* **218**, 1089–1099 (2019).
87. Liu, J.-L., Qian, W.-C., Guo, J.-Z., Shen, Y. & Li, B. Selective removal of anionic and cationic dyes by magnetic Fe_3O_4-loaded amine-modified hydrochar. *Bioresour. Technol.* **320**, 124374 (2021).
88. Lin, C., Dong, B. & Xu, Z. Competitive adsorption of heavy metals onto xanthate-modified sludge hydrochar and its solidification as secondary minerals. *Chemosphere* **356**, 141878 (2024).
89. Huang, X. et al. Magnetic hydrochar from the extract and residue of herbal medicines for adsorption and Fenton reaction. *Powder Technol.* **427**, 118636 (2023).
90. Algethami, J. S., Alhamami, M. A. M., Alqadami, A. A., Melhi, S. & Seliem, A. F. Magnetic hydrochar grafted-chitosan for enhanced efficient adsorption of malachite green dye from aqueous solutions: Modeling, adsorption behavior, and mechanism analysis. *Int. J. Biol. Macromol.* **254**, 127767 (2024).
91. Zhu, J. Utilization of peanut hull hydrochar/beta cyclodextrin/Fe_3O_4 magnetic composite for lead ion removal from water solution. *Environ. Res.* **259**, 119525 (2024).
92. Qiao, Y., Liu, X., Zhu, H., Zhang, S. & Shen, L. $KMnO_4$ modified magnetic hydrochar for efficient adsorption of malachite green and methylene blue from the aquatic environment. *J. Ind. Eng. Chem.* https://doi.org/10.1016/j.jiec.2024.05.007 (2024).
93. Pei, T. et al. Bamboo-derived nitrogen-doping magnetic porous hydrochar coactivated by K_2FeO_4 and $CaCO_3$ for phenol removal: governing factors and mechanisms. *Environ. Pollut.* **331**, 121871 (2023).
94. Wang, F. et al. A novel cobalt-iron bimetallic hydrochar for the degradation of triclosan in the aqueous solution: performance, reusability, and synergistic degradation mechanism. *Environ. Pollut.* **358**, 124487 (2024).
95. Zhang, J. et al. Ultra-fast degradation of ciprofloxacin by the peroxymonosulfate activation using a Co/Al-LDH decorated magnetic hydrochar: structural design, catalytic performance and synergistic effects. *Chem. Eng. J.* **477**, 146961 (2023).
96. Di Caprio, F. et al. Two-phase synthesis of Fe-loaded hydrochar for as removal: the distinct effects of initial pH, reaction time and Fe/hydrochar ratio. *J. Environ. Manag.* **302**, 114058 (2022).
97. Yan, W., Zhang, H., Sheng, K., Mustafa, A. M. & Yu, Y. Evaluation of engineered hydrochar from $KMnO_4$ treated bamboo residues: physicochemical properties, hygroscopic dynamics, and morphology. *Bioresour. Technol.* **250**, 806–811 (2018).
98. Zhu, X., Qian, F., Liu, Y., Zhang, S. & Chen, J. Environmental performances of hydrochar-derived magnetic carbon composite affected by its carbonaceous precursor. *RSC Adv.* **5**, 60713–60722 (2015).
99. Qu, J. et al. Pinecone-derived magnetic porous hydrochar co-activated by $KHCO_3$ and K_2FeO_4 for Cr(VI) and anthracene removal from water. *Environ. Pollut.* **306**, 119457 (2022).
100. Siddiqui, M. T. H. et al. Comparative study of microwave and conventional solvothermal synthesis for magnetic carbon nanocomposites and bio-oil from rice husk. *J. Environ. Chem. Eng.* **7**, 103266 (2019).

101. Qu, J. et al. Microwave-assisted one-pot preparation of magnetic cactus-derived hydrochar for efficient removal of lead(II) and phenol from water: performance and mechanism exploration. *Bioresour. Technol.* **388**, 129789 (2023).
102. Purnomo, C. W., Castello, D. & Fiori, L. Granular activated carbon from grape seeds hydrothermal char. *Appl. Sci.* **8**, 331 (2018).
103. Wu, K., Zhang, X., Li, X., Yuan, Q. & Liu, R. Investigation of hydrochar properties and bio-oil composition from two-stage hydrothermal treatment of dairy manure. *Fuel* **339**, 126945 (2023).
104. Chen, Z. et al. Emerging adsorbents for micro/nanoplastics removal from contaminated water: advances and perspectives. *J. Clean. Prod.* **371**, 133676 (2022).
105. Zhu, X. et al. Facile fabrication of magnetic carbon composites from hydrochar via simultaneous activation and magnetization for triclosan adsorption. *Environ. Sci. Technol.* **48**, 5840–5848 (2014).
106. Yu, Z. et al. Ultra-high adsorption of CR from aqueous solution using LDHs decorated magnetic hydrochar: selectivity and anti-interference exploration. *Sep. Purif. Technol.* **313**, 123438 (2023).
107. Zhang, F. et al. Effective removal of tetracycline antibiotics from water by magnetic functionalized biochar derived from rice waste. *Environ. Pollut.* **330**, 121681 (2023).
108. Yang, X., Wang, B. & Cheng, F. Adsorption performance on tetracycline by novel magnetic adsorbent derived from hydrochar of low-rank coal and sewage sludge. *Sep. Purif. Technol.* **330**, 125482 (2024).
109. Qu, J. et al. A novel PEI-grafted N-doping magnetic hydrochar for enhanced scavenging of BPA and Cr(VI) from aqueous phase. *Environ. Pollut.* **321**, 121142 (2023).
110. Luo, X. et al. Enhanced adsorption and co-adsorption of heavy metals using highly hydrophilicity amine-functionalized magnetic hydrochar supported MIL-53(Fe)-NH_2: performance, kinetics, and mechanism studies. *Environ. Sci. Pollut. Res.* **30**, 76204–76216 (2023).
111. Minale, M. et al. Insight into adsorption behavior of chlortetracycline and cadmium in aqueous solution using a novel manganese ferrite loaded swine manure hydrochar. *J. Environ. Chem. Eng.* **9**, 106785 (2021).
112. Siddiqui, M. T. H. et al. Synthesis and optimization of chitosan supported magnetic carbon bio-nanocomposites and bio-oil production by solvothermal carbonization co-precipitation for advanced energy applications. *Renew. Energy* **178**, 587–599 (2021).
113. Qu, J. et al. One-pot synthesis of Ca-based magnetic hydrochar derived from consecutive hydrothermal and pyrolysis processing of bamboo for high-performance scavenging of Pb(II) and tetracycline from water. *Bioresour. Technol.* **343**, 126046 (2022).
114. Cui, T. et al. Chromium immobilization from wastewater via iron-modified hydrochar: different iron fabricants and practicality assessment. *Ecotoxicol. Environ. Saf.* **274**, 116132 (2024).
115. Kazak, O. & Tor, A. In situ preparation of magnetic hydrochar by co-hydrothermal treatment of waste vinasse with red mud and its adsorption property for Pb(II) in aqueous solution. *J. Hazard. Mater.* **393**, 122391 (2020).
116. Nassar, A. E., El-Aswar, E. I., Rizk, S. A., Gaber, S. E.-S. & Jahin, H. S. Microwave-assisted hydrothermal preparation of magnetic hydrochar for the removal of organophosphorus insecticides from aqueous solutions. *Sep. Purif. Technol.* **306**, 122569 (2023).
117. Wang, H. et al. Simultaneously cationic and anionic dyes elimination via magnetic hydrochar prepared from copper slag and pinewood sawdust. *Toxics* **11**, 484 (2023).
118. Chauhan, C. et al. Unveiling the potential of Rhododendron foliage: a novel eco-friendly and cost-effective approach for cationic dye removal using in situ co-hydrothermally synthesized magnetic hydrochar. *Biomass Convers. Biorefinery*, https://doi.org/10.1007/s13399-024-05873-y (2024).
119. M Khairy, G., Hesham, A. M., Jahin, H. E. S., El-Korashy, S. A. & Mahmoud Awad, Y. Green synthesis of a novel eco-friendly hydrochar from Pomegranate peels loaded with iron nanoparticles for the removal of copper ions and methylene blue from aqueous solutions. *J. Mol. Liq.* **368**, 120722 (2022).
120. Qu, J. et al. Removal of Cd(II) and anthracene from water by β-cyclodextrin functionalized magnetic hydrochar: performance, mechanism and recovery. *Bioresour. Technol.* **337**, 125428 (2021).
121. Algethami, J. S., Alhamami, M. A. M., Alqadami, A. A., Melhi, S. & Seliem, A. F. Adsorptive performance of a new magnetic hydrochar nanocomposite for highly efficient removal of cadmium ions from water: mechanism, modeling, and reusability studies. *Environ. Technol. Innov.* **32**, 103404 (2023).
122. Chen, H. et al. Arsenic removal via a novel hydrochar from livestock waste co-activated with thiourea and γ-Fe_2O_3 nanoparticles. *J. Hazard. Mater.* **419**, 126457 (2021).
123. Khan, M. A. et al. Oil industry waste based non-magnetic and magnetic hydrochar to sequester potentially toxic post-transition metal ions from water. *J. Hazard. Mater.* **400**, 123247 (2020).
124. Zhang, Y. et al. Simultaneous scavenging of Cd(II) and Pb(II) from water by sulfide-modified magnetic pinecone-derived hydrochar. *J. Clean. Prod.* **341**, 130758 (2022).
125. Wang, H. et al. Magnetic hydrochar derived from waste lignin for thallium removal from wastewater: performance and mechanisms. *Bioresour. Technol.* **374**, 128736 (2023).
126. Zou, W. et al. Hydroxylamine mediated Fenton-like interfacial reaction dynamics on sea urchin-like catalyst derived from spent $LiFePO_4$ battery. *J. Hazard. Mater.* **431**, 128590 (2022).
127. Liu, X. et al. Persistent free radicals on biochar for its catalytic capability: a review. *Water Res.* **250**, 120999 (2024).
128. Li, H. et al. Highly efficient removal of thallium(I) from wastewater via hypochlorite catalytic oxidation coupled with adsorption by hydrochar coated nickel ferrite composite. *J. Hazard. Mater.* **388**, 122016 (2020).
129. Zhang, C. et al. Reuse of microalgae residue after oil production as a Fenton-like catalyst in wastewater treatment: catalytic performance and mechanism. *J. Water Process Eng.* **55**, 104092 (2023).
130. Tu, Y. et al. Preparation and characterization of magnetic biochar nanocomposites via a modified solvothermal method and their use as efficient heterogeneous Fenton-like catalysts. *Ind. Eng. Chem. Res.* **59**, 1809–1821 (2020).
131. Qian, J. et al. Sulfur-decorated Fe/C composite synthesized from MIL-88A(Fe) for peroxymonosulfate activation towards tetracycline degradation: multiple active sites and non-radical pathway dominated mechanism. *J. Environ. Manag.* **344**, 118440 (2023).
132. Geçgel, C., Yabalak, E. & Turabik, M. Simultaneous synthesis of super-paramagnetic hydrochar in a one-pot using subcritical water medium and evaluation of its photocatalytic activity. *J. Environ. Manag.* **362**, 121333 (2024).
133. Li, S. et al. Hydrochar-mediated photocatalyst Fe_3O_4/BiOBr@HC for highly efficient carbamazepine degradation under visible LED light irradiation. *Chem. Eng. J.* **433**, 134492 (2022).
134. Chen, N., Huang, Y., Hou, X., Ai, Z. & Zhang, L. Photochemistry of hydrochar: reactive oxygen species generation and sulfadimidine degradation. *Environ. Sci. Technol.* **51**, 11278–11287 (2017).
135. Marzban, N. et al. Hydrochar stability: understanding the role of moisture, time and temperature in its physiochemical changes. *Biochar* **6**, 38 (2024).
136. Zhang, B. et al. Sewage sludge valorisation by hydrothermal carbonization: a new method to enhance nitrogen removal in hydrochar catalyzed with Ni-Mg-Al layered double oxides. *J. Clean. Prod.* **386**, 135880 (2023).
137. Elshishini, H. M., Elsubruiti, G. M., Ghatass, Z. F. & Eltaweil, A. S. Microwave-assisted synthesis of Zn–Fe LDH modified with magnetic oxidized hydrochar for Pb(II) removal: insights into stability, performance and mechanism. *J. Solid State Chem.* **335**, 124689 (2024).

138. Farru, G. et al. Benefits and limitations of using hydrochars from organic residues as replacement for peat on growing media. *Horticulturae* **8**, 325 (2022).
139. Sun, Y., Wang, T., Han, C., Bai, L. & Sun, X. One-step preparation of lignin-based magnetic biochar as bifunctional material for the efficient removal of Cr(VI) and Congo red: performance and practical application. *Bioresour. Technol.* **369**, 128373 (2023).
140. Idowu, I. et al. Hydrothermal carbonization of food waste for nutrient recovery and reuse. *Waste Manag.* **69**, 480–491 (2017).
141. Schulze, M., Mumme, J., Funke, A. & Kern, J. Effects of selected process conditions on the stability of hydrochar in low-carbon sandy soil. *Geoderma* **267**, 137–145 (2016).
142. Flora, J. F. R., Lu, X., Li, L., Flora, J. R. V. & Berge, N. D. The effects of alkalinity and acidity of process water and hydrochar washing on the adsorption of atrazine on hydrothermally produced hydrochar. *Chemosphere* **93**, 1989–1996 (2013).
143. Juturu, R., Selvaraj, R. & Murty, V. R. Efficient removal of hexavalent chromium from wastewater using a novel magnetic biochar composite adsorbent. *J. Water Process Eng.* **66**, 105908 (2024).
144. Deng, F. et al. Hydrothermally treated peat/magnetite composites as highly efficient heterogeneous Fenton catalyst: integrating multiple reaction mechanisms to enhance the catalytic reactivity for BPA removal. *Chem. Eng. J.* **473**, 144946 (2023).
145. Zhong, J. et al. Hydrothermal carbonization of coking sludge: migration behavior of heavy metals and magnetic separation performance of hydrochar. *J. Environ. Chem. Eng.* **12**, 114141 (2024).
146. Baskar, A. V. et al. Recovery, regeneration and sustainable management of spent adsorbents from wastewater treatment streams: a review. *Sci. Total Environ.* **822**, 153555 (2022).
147. Liu, H. et al. A life cycle assessment of hard carbon anodes for sodium-ion batteries. *Philos. Trans. R. Soc. A: Math., Phys. Eng. Sci.* **379**, 20200340 (2021).
148. Berge, N. D., Li, L., Flora, J. R. V. & Ro, K. S. Assessing the environmental impact of energy production from hydrochar generated via hydrothermal carbonization of food wastes. *Waste Manag.* **43**, 203–217 (2015).
149. Kaboggoza, H. C., Muoghalu, C., Sprouse, L. & Manga, M. Hydrochar composites for healthcare wastewater treatment: a review of synthesis approaches, mechanisms, and influencing factors. *J. Water Process Eng.* **60**, 105222 (2024).

Acknowledgements

This work was supported by the Australian Research Council (ARC) Discovery Projects (DP220101139 and DP220101142).

Author contributions

H.S.M. wrote the initial manuscript, prepared the figures, and edited the final draft. Z.J.C. contributed to the conceptualization and writing of the manuscript. W.W., H.R.D., and M.Z. contributed to the review process. J.X. and B.J.N. contributed to the review, editing, and supervision.

Competing interests

The authors declare no competing interests.

Additional information

Correspondence and requests for materials should be addressed to Zhijie Chen, Juan Xu or Bing-Jie Ni.